
# UNIVERSITA' POLITECNICA DELLE MARCHE
# FACOLTA' DI MEDICINA E CHIRURGIA

**Dottorato di Ricerca XXXII CICLO**

**in**

**SCIENZE BIOMEDICHE**

## PANCREATIC DUCTAL ADENOCARCINOMA: MICROENVIRONMENT AND

## CLINICAL FINDINGS

Relatore:

Prof. Giovanni Principato

Dottoranda:

Dr.ssa Alessandra Righetti

Correlatore:

Dott. Francesco Piva

Anno Accademico 2018-2019

**TABLE OF CONTENT**

# 1. INTRODUCTION

## 1.1 Pancreatic Tumour

Pancreas is an abdominal glandular organ, 15cm long, in close contact with stomach, spleen, liver, small intestine and spinal column. There are two components of pancreas:

- Exocrine: produces different digestive enzymes (such as amylase, lipase and protease) which through pancreatic ducts are released inside the intestine and contribute to processes of digestion and absorption.

- Endocrine: produces and releases many hormones (insulin, glucagon, somatostatin) that regulate blood sugar metabolism.

Two types of cancer may affect pancreas: pancreatic neuroendocrine cancer, infrequent (about 5%) due to the pancreas endocrine portion, and pancreatic ductal adenocarcinoma (PDAC) which is the most common type. The latter is often located at the pancreas head portion, is about 70% of pancreas tumour cases and originates in the organs exocrine portion, in particular inside ducts which transport digestive enzymes [1].

Pancreatic ductal adenocarcinoma is one of the most malignant tumours of the gastrointestinal system and is considered the seventh leading cause of cancer death in the world, with a 5-year survival rate of less than 5%. In fact, over the next 20 years its incidence is estimated to increase and will include about 300,000 new cases [2].

Usually, the modification that affects pancreatic ducts is called PanIN (Pancreatic Intraductal Neoplasia) to describe pancreatic intraductal alterations. In tumour progression, ducts undergo various morphological changes and based on these different modifications, may be classified adenocarcinoma into:

- Type I PanIN: the tumour is limited to the pancreas (there is no diffusion and the tumour is resectable) its size is about 2cm (Type IA), the cells from cubic are transformed into columns. If the tumour is larger than 2cm, but less than 4cm it is defined as type IB and there is a papillary extroflexion of the typical columnar epithelium.

- PanIN type II: the carcinoma diffusion is limited to the pancreas or to the nearby lymph nodes, this type of tumour is greater than 4 cm. In this situation the tumour is borderline resecable. Their cells present nuclear atypia and pluristratification.

- PanIN type III: the carcinoma reached blood vessels or neighbouring nerves, but it has not yet metastasized in distant sites; the tumour at this point is not resectable. The ductal epithelium is characterized by a swelling, there is a loss of cell polarity and a sclerotic tissue surround the tissue.

- PanIN type IV: carcinoma is extended to distant organs and has acquired a metastatic phenotype.

Pancreatic cancer is often impossible to diagnose in early stages, and this is probably due to its anatomical position and the lack of specific symptoms. From the anatomical point of view, the pancreas is positioned behind other organs, such as the stomach, small intestine, bile ducts, gall bladder, liver and spleen, therefore it is not sensitive to compression and does not allow to verify a possible change in size. As for the symptoms, however, in the initial stages very often this tumour is asymptomatic or presents non-specific symptoms such as abdominal pain, weight loss, nausea, vomiting, lethargy and icterus. In more than 80% of patients, the tumour is then diagnosed at an advanced stage, which unable surgical resection, due to vascular invasion or presence of distant metastases [2, 3]. Unfortunately, diagnostic tests are not yet available to identify the early stages of pancreatic ductal adenocarcinoma. Surgical resection, chemotherapy and radiotherapy treatments are used to extend patient survival and alleviate symptoms [2]. Unfortunately, even for patients who have undergone radical surgery, the 5-year survival rate is about 25%. In most cases the recurrence rate within one year is 54% followed by metastases and resistance to chemotherapy and radiotherapy [4, 5]. Currently, there is still not a definitive cure, therefore, a screening program is urgently needed in order to develop an early diagnosis approach of pancreatic cancer [2, 4].

### 1.1.1 Risk factors

Nowadays, although the main causes of pancreatic cancer are still unknown, some risk factors have been identified. These have been classified into two categories, as listed below [6, 7].

- Modifiable risk factors: i) Smoking: tobacco smoke is considered one of the most important factors leading to the onset of pancreatic cancer. Usually, smokers are 75% more likely to develop the disease than non-smokers and even up to 8-10 years after they quit smoking, they might develop cancer. Obviously, if the 5 cigarettes are exceeded daily, this incidence increases. The PDAC incidence is also high, 50%, for individuals exposed to passive smoking. After 10 years of quitting smoking, the incidence of PDAC decreases. Daily alcohol consumption, either alone or in association with smoking, is associated with higher mortality in PDAC [2, 6, 8]. ii) Diet and Obesity: a correlation was found between the consumption of cholesterol-rich foods, processed meats, red-meats, etc. and a cancer incidence, which is increased with consumption increase. Unlike, consuming foods with antioxidant activity, seems to have a protective action. It has also been seen that the continuous intake of processed foods and the lack of physical activity can contribute to the accumulation

of fat and can lead to the onset of obesity. This condition would significantly increase the risk of developing PDAC and is also associated with a mortality increase [2, 6, 8]. iii) Occupational Exposures to Toxic Substances: there are many toxic substances present in work environments that can be dangerous and lead to cancer development. For example, in the case of PDAC, nickel can increase DNA methylation, inhibit its repair and, through the formation of ROS, induce apoptosis. In addition to nickel, cadmium and selenium have also been associated with the onset of PDAC [2].

- Unchangeable risk factors: i) Sun exposure: studies carried on populations in northern Europe, Scandinavia and northern Japan, shown that sun exposure would decrease the PDAC mortality. In fact, it would seem that the absorption of vitamin D, following solar exposure, has a protective role in relation to PDAC. These data, however, must be confirmed [8]. ii) Sex, Age and Ethnicity: most frequently, pancreatic cancer occurs in male individuals. On one hand, this factor could be due to environmental and/or professional risk factors and different lifestyles, such as the higher consumption of alcohol or smoking, on the other hand it might be due to genetic factors that can affect PDAC onset and mortality. Age between 60 and 80 years is the typical period in which tumour occurs. Sometimes, in heavy smokers, in patients who have PDAC family history and in patients who are undergoing radiation therapy for another tumour, PDAC can occur early (before the age of 50). From an ethnic point of view, Caucasians present a lower risk of PDAC than african-americans. Diet, smoking, alcohol and genetics are all factors to be attributed to this difference [2, 6, 8]. iii) Family history: 10% of PDAC occurs in subjects with a previous history of family pancreatic cancer. These individuals in fact, present a 9 times greater risk of developing PDAC, compared to those who do not have a first degree relative who developed the disease. The incidence of disease development increases if the relative has had the disease before the age of 50 [2, 6]. iv) Diabetes mellitus and Chronic pancreatitis: the first is considered an important factor having a dual role in relation to PDAC. In fact, the diabetes mellitus, it can both be a risk factor for the onset and can be considered a useful marker to identify the presence of pancreatic cancer. In fact, in most cases this pathology occurs following the development of pancreatic cancer. In about 4% of individuals with chronic pancreatitis, pancreatic adenocarcinoma develops later. Pancreas chronic inflammations can lead to the accumulation of ROS, to chromosomal instability and other factors that can trigger the onset of PDAC [2, 6, 8].

### 1.1.2 Mutations

Pancreatic ductal adenocarcinoma is characterized by many genetic alterations which play an important role in tumour development and progression. Up to 10% of these alterations is constituted by hereditary gene mutations, while the high percentage is somatic genetic alterations. Numerous genes have been identified in PDAC pathogenesis. Among these, mutations affecting the K-Ras proto-oncogenic gene and the tumour suppressor genes SMAD4, TP53 and p16, are those most commonly found in PDAC progression [4, 5, 9]. In 80-100% of PDAC patients, the following gene alterations were found [8]:

- Point mutations activating the K-ras oncogene: K-ras is a gene that codes for a small GTPase protein of 21 KDa that controls cell proliferation and survival. Physiologically it is in a quiescent state linked to GDP (which replaces GTP when growth factors bind to its receptors). The Kras activating point mutations, which occur in codon 12 (in particular G12, G13 and Q61), mean that RAS is no longer susceptible to GAPs, and involves an inhibition of GTP hydrolysis. This process causes a constant activation of RAS [10]. These mutations are found in 90-100% of PDAC patients [9], and typically occur in early low-grade PanIN-I lesions. The K-Ras protein is responsible for activating a series of signalling pathways, such as MAPK/ERK, PI3K, RalGDS pathways, which cause tumour progression [4, 8].
- p16 onco-suppressor loss: In 95% of PDAC patients, "germline mutation" causes inactivation of the CDK2NA tumour suppressor gene (also called p16), which encodes an essential cell cycle regulator. Normally, this gene, located on chromosome 9, inhibits cell cycle progression by intervening during the G1-S checkpoint. Its inactivation involves an uncontrolled cell growth and an inappropriate progression through the cell cycle. CDK2NA alterations are early events found in PanIN-II pre-neoplastic lesions [4, 10].
- Loss of the on-board suppressor p53: located on chromosome 17, TP53 gene encodes a protein that plays a key role in the response to cellular stress. In a physiological state, TP53 is activated following the presence of cellular stress and / or DNA damage. This activation induces cell cycle arrest, repair of DNA damage, senescence and apoptosis [8, 10]. The loss of TP53 function during carcinogenesis leads to an uncontrolled cell growth that increases genetic instability. In 75-80% of PDAC patients' missense mutations against TP53 produce a non-functional full-length protein; these mutations are found in the PanIN-III lesions [4, 9].
- Inactivating mutations at SMAD4 level: present on chromosome 18, SMAD4 is a tumour suppressor, downstream TGF-β effector and acts in the nucleus as a transcription factor that promotes growth inhibition. In about 55% of PDAC cases, SMAD4 is inactivated, in 30% it is deleted in heterozygosity, in the remaining cases it is mutated [4, 9, 10].

### 1.2 Tumour Microenvironment

To understand the mechanisms underlying the processes of development and progression of pancreatic ductal adenocarcinoma, it is fundamental to study the role of the tumour microenvironment. In fact, this dense fibrotic stroma is not static, but it is constantly changing as the tumour progresses. Within this microenvironment, tumour cells can interact with both other tumour cells and factors that are part of the microenvironment itself. This interaction allows a continuous exchange of information between tumour cells and stromal cells, and favours their proliferation, migration and even resistance to chemotherapy drugs [11-13].

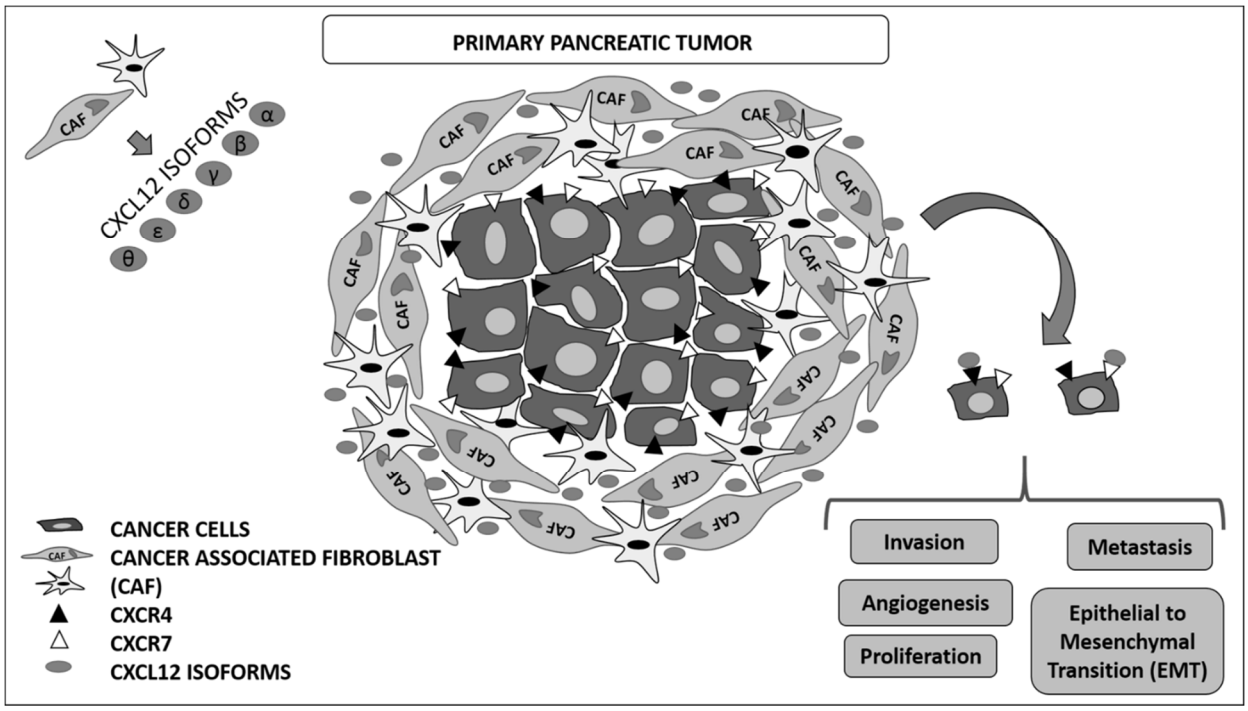


***Figure 1.*** *PDAC microenvironment [14].*

In pancreatic ductal adenocarcinoma, tumour cells represent a small part of the tumour mass. This dense and fibrous microenvironment is particularly heterogeneous and composition differs upon PDAC progress from pre-neoplastic PanIN to invasive cancer [13]. The PDAC stroma consists of a cellular component and a non-cellular component: the first comprises fibroblasts, immune cells, pancreatic stellate cells, endothelial cells, inflammatory cells, hematopoietic cells, blood vessel and nerve cells; the second comprises extracellular matrix (ECM), including collagens, non-collagen glycoproteins, glycosaminoglycans, growth factors, proteoglycans and modulators of cell-matrix interaction [15, 16].

These components constitute the desmoplasia that characterizes the PDAC by forming a compact barrier that does not allow the entry of chemotherapeutic drugs and contributes to the cancer development [17]. The 50% of this stroma is made up of tumour-associated fibroblasts (CAF). These CAFs, through the secretion of proteins and inflammatory cytokines, promote tumour growth [15].

Furthermore, again by releasing these factors, CAFs modulate the inflammatory response, removing the recalled T cells from the tumour site and promoting an immunosuppressive state [7, 16]. In TME there are also numerous CAFs that express FAP proteins, which support migration and PDAC proliferation [15].

Stellate pancreatic cells (PSCs), so named because of their stellate form, are the most studied subtype of CAFs. Under normal conditions they are in a quiescent state and are characterized by the presence of long cytoplasmic extensions and lipid vitamin A droplets. In an inflammatory or tumorigenic state, however, these cells are activated and take on a myofibroblast phenotype by upregulation of aSMA (smooth muscle) actin and collagen I. PSCs produce a high quantity of ECM molecules, such as laminin, fibronectin and periostin which promote pancreatic fibrosis. In addition to increasing nucleus size, they also loose fat droplets containing vitamin A. These factors cause an increase in cell proliferation with consequent promotion of tumour growth [15, 17-19].

Immune cells, such as tumour-associated macrophages (TAM), are also present within the PDAC microenvironment. These cells, which can be found infiltrated inside the tumour, represent a rich source of growth factors, such as: HGF, TGF and EGF. By producing MMP9 and other factors, they stimulate proliferation, angiogenesis and EMT.

The combination of all these factors favours the development and invasion of the PDAC. In fact, these mechanisms protect tumour cells from the host's immune system, allowing both the development of resistance to chemotherapeutic drugs and the possible formation of niches favourable for metastases development [12, 20].

The interaction between the multiple cell types that make up the pancreatic tumour microenvironment is allowed by the release of numerous components, such as: growth factors (FGF, EGF, VEGF and HGF), cytokines, chemokines and also by release of vesicles secreted by the extracellular matrix, the exosomes. In this interaction, the tumour cells release signals capable of controlling the stromal component, while all these released molecules (chemokines, exosomes, growth factors, etc.) take part in the processes of growth, invasion and migration of these tumour cells, thus favouring the uncontrolled growth of the tumour mass [12].

### 1.2.1 CXCL12

Chemokines, low molecular weight proteins, have aroused particular interest through many signals released inside the PDAC tumour microenvironment. Numerous studies have shown that these

proteins, generating a gradient able to recall immune-system cells into the site of infection, can be actively involved in processes like embryogenesis, angiogenesis and chemotaxis.

Also, in tumour development processes, these signalling molecules appear to have an essential role; their expression shows a clear correlation with the increase of malignant cells in giving rise to metastases [21].

In particular, among chemokines it was discovered CXCL12 protein, highly secreted by the stellate cells of PDAC microenvironment, which in addition to being an important signal in biological processes, plays a messenger role both among tumour cells and between tumours and stromal cells. In fact, CXCL12 mediate the communication between cells of the tumour microenvironment favouring the growth and development of pancreatic ductal adenocarcinoma 29082918 [14, 22, 23]. This growth is favoured by the CXCL12 binding to one of its receptors, CXCR4 or ACKR3, highly expressed on the tumour cells surface. The ligand-receptor interaction leads to the activation of one or more signalling pathways, with the consequent onset of a tumorigenic phenotype [14, 24-26].

The CXCL12 binding to CXCR4 receptor, involves the activation of several signalling pathways, related to tumour progression, survival and development, such as: phospholipase C, MAPK, and PI3K-Akt-mTOR pathways [14, 22, 27, 28]. On the other hand, the role of ACKR3 receptor is not entirely clear. It seems, in fact, that on the one hand, by means of β-arrestin it activates a pro-tumour signalling pathway [29], on the other hand, by subtracting CXCL12 from the extracellular environment and consequently preventing its binding with CXCR4, it can have an anti-tumour function [30].

Seven different CXCL12 isoforms have been currently identified: α-isoform, β-isoform, γ-isoform, δ-isoform, ε-isoform, θ isoform-θ and a seventh isoform which has only been predicted.

All isoforms are released as pro-peptides and in order to be active, therefore able to bind to the receptor, they are subsequently subjected to the proteolytic cutting of 21 amino acids at the N-terminal end. The protein active form presents the first 8AA, in the N-terminal region, with a specific role in ligand-receptor interaction. In particular, the first two AAs activate the receptor, while the remaining 6 AA mediate the ligand-receptor bond.

The seven different CXCL12 isoforms share all the first 3 exons (1-68AA) and due to the length of the fourth exon they differ in length from one another: 89 AA isoform-α, 93 AA isoform- β, 119 AA the isoform-γ, 140 AA the isoform-δ, 90 AA the isoform-ε and 100 AA the isoform-θ.

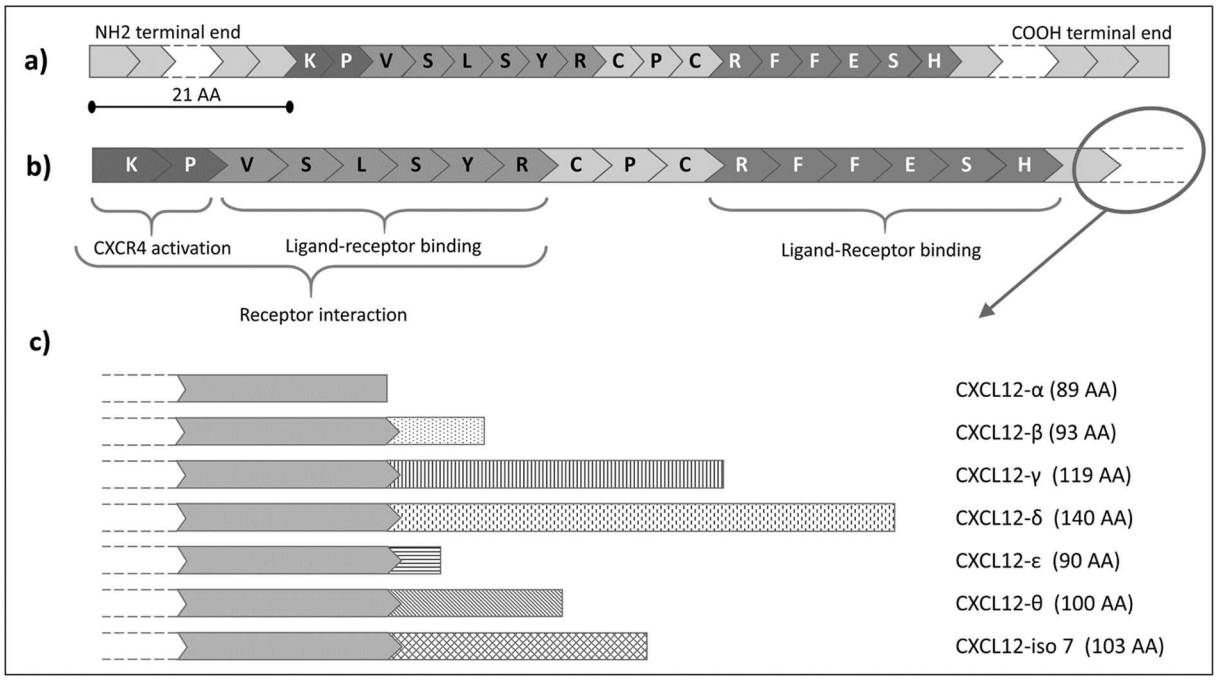


***Figure 2**. CXCL12 chemokine: a) CXCL12 immature sequence; b) CXCL12 sequence after proteolytic cutting; c) different CXCL12 isoforms [14].*

The specific role of each variant has not yet been investigated, however, they appear to have different functions one from another and different expression levels. Different involvement of each isoform in numerous neoplastic processes has also been hypothesized. In fact, low levels of isoform-α expression correlate with lower survival rate in breast cancer. Also, low expression levels of β-isoform are associated with poor prognosis in breast cancer [31], as well as mRNA levels in bladder cancer [32]. Concerning CXCL12-γ, its high expression levels in breast cancer are positively associated with patient survival, as well as tumour size for colorectal carcinoma [31, 33]. Furthermore, the γ-isoform, in prostate cancer, plays a key role in promoting a neoplastic phenotype [34].

Little is known about the other CXCL12 isoforms, only that an over-expression of the δ-isoform appears to be related to better survival rate n breast cancer [31].

Among data reported in the literature, it is not often clearly indicated which type of CXCL12 isoform has been used. In fact, each of them could play a pro-tumoural role, favouring tumour growth, or, on the contrary, could have an anti-tumour role by inhibiting the progression of pancreatic ductal adenocarcinoma. It is therefore interesting to conduct further investigations to understand how each isoform acts within the tumour microenvironment.

### 1.2.2 EXOSOMES

Exosomes are small extracellular vesicles, about 100nm in diameter, which are constantly being released from all cells and are present in all body fluids. These vesicles, due to their small size and their content in tetraspanins and rab proteins, are different from other classes of micro-vesicles. From the biogenesis point of view, micro-vesicles derive from direct extrusion of plasma cell membrane, exosomes, instead, derive from recycling of the multi-vesicular bodies [35, 36].

To date, it is not yet known what are the factors that stimulate the cell to selectively release exosomes, but the interest in these particles is increasingly growing since it is known that they are excellent tools that mediate cell-cell signalling, within the body, and even between tissues belonging to districts very far from each other. In fact, thanks to their ability to fuse with other cells, exosomes are able to achieve distance communication, in other words they allow an exchange of cell-cell information [37].

In addition to role in numerous physiological processes, communication mechanism implemented by exosomes plays a key role in many pathological processes, such as inflammation and tumorigenesis. In fact, there is important evidence that this signalling mechanism can determine the maintenance of the tumour microenvironment, by supporting hypoxia, the mesenchymal epithelial transition (EMT), as well as favouring tumour progression through the formation of pre-metastatic niches or by immuno-escape [37-39].

Thanks to the information contained in exosomes, in the form of proteins, lipids, nucleic acids and micro-RNAs, the interest in these nano-particles is increasingly growing. Released by a cell of origin, they send a message by specifically fusing with a receiving cell [39].

In tumour microenvironment, it has been shown that tumour-associated fibroblasts (CAF), treated with gemcitabine, release exosomes capable of inducing proliferation and survival of pancreatic cancer cells. Increased levels of miR-146a and Snail in recipient cells promote this phenomenon. If the release of exosomes is reduced, the progression of cancer cells is also reduced [40]. Another study found that the release of exosomes from highly malignant pancreatic cancer cells stimulates proliferation, invasion and migration of moderately malignant cancer cells. In this case, the ZIP4 transporter appears to be the main protein involved, up-regulated in moderately malignant cells [41].

In pancreatic ductal adenocarcinoma, exosomes have been shown to play an important role in activating or suppressing the immune system, and the idea of using them as nano-carriers in immunotherapy drugs [37, 42] has been proposed. Likewise, in a study concerning the PDAC microenvironment, it was seen that tumour microenvironment is characterized by a high accumulation of T-Reg cells and minimal infiltration of immune cells CD8 + T [43, 44]. This condition, in patients with melanoma, is due to the presence, in bloodstream, of PDL1-positive exosomes that block the

proliferation and infiltration of the CD8 + T cells in the tumour microenvironment. The presence of these exosomes, if confirmed also in the pancreas, could be useful to implement a specific therapy in the treatment of PDAC tumour [37, 45].

Exosomes released from pancreatic cancer cells can also induce a change of macrophages towards a pro-tumoral phenotype. Furthermore, these macrophages, if treated with exosomes extracted from PDAC cell lines, induce a massive release of cytokines and growth factors, favouring the progression, invasion and metastasis of pancreatic cancer [46]. Finally, exosomes, through their content in micro-RNA and proteins, are able to induce chemoresistance in pancreatic cancer. In particular, the release of miR-21 exosomes by CAFs stimulates the activation of the PI3K/AKT or APAF1 pathways inducing chemoresistance [47, 48].

Because of their involvement in numerous PDAC tumorigenesis processes, exosomes are considered as potential tumour bio-markers. If it was possible to correlate which subpopulations of exosomes are released in the different stages of progression of pancreatic ductal adenocarcinoma, these exosomes, easily found by liquid biopsy, would be very useful for early detection of the disease.

## 2. AIMS OF THE THESIS

### 2.1 CXCL12

Within the tumour microenvironment, the tumour cells survival is favoured by the constant tumour-stroma interaction. Released by the cancer associated fibroblast (CAF), the chemokine CXCL12, plays a controversial role in regulating tumour behaviour. In fact, sometimes a pro-tumour role of CXCL12 and other times an anti-tumour role emerges. In humans, seven different CXCL12 isoforms have been discovered and probably each of them has a different and specific function. Until now, commercial products containing a mixture of multiple CXCL12 isoforms were used and each isoforms function were never being evaluated. The single role of the 7 CXCL12 isoforms has never been evaluated, in fact, in all the experiments performed the CXCL12 product was used as if there were only one protein form. Since, in pancreatic cancer, it has been hypothesized that the cause of the contradictory results related to CXCL12 function is likely due to the different role of each isoform, the purpose of this thesis is to determine the specific role of each CXCL12 isoform in PDAC. In particular, the pro-tumour or the anti-tumour effect of the commercially available isoforms, CXCL12-α, CXCL12-β and CXCL12-γ, have been evaluated on the h-Tert HPNE pre-tumour pancreatic cell line.

### 2.2 EXOSOMES

Since cells at different times release exosomes with different content, the aim of this work is to verify the existence of correlations between exosomes subpopulations released in PDAC plasma patients and their clinical variables. This work has also been carried out in order to verify if these subpopulations could constitute possible prognostic biomarkers.

## 3. MATERIALS AND METHODS

### 3.1 CXCL12

#### 3.1.1 Cell cultures

For this study the following cell line were chosen: hTERT-HPNE. The human pancreatic pre-tumour cell line hTERT-HPNE E6/E7/K-RasG12D (ATCC® CRL-4038™) were purchased from American Type Culture Collection (ATCC). This cell line derives from normal pancreas ductal epithelial cells. It has a telomerase catalytic component (hTERT) that is able to restore the DNA base pairs lost from the telomeres during cell divisions. Therefore, the chromosomal length is maintained constant and cells continue to divide without becoming senescent. The hTERT-HPNE E6/E7/K-RasG12D cell line resembles normal pancreatic cells in-vivo in terms of physiological properties, retains the expression of phenotypic markers and has a stable diploid karyotype. This is in contrast to many traditional immortalized cell lines, which are known to develop an unstable karyotype, especially at high passage numbers and when oncogenes are used. Moreover, the hTERT-HPNE E6/E7/K-RasG12D retains anchorage dependent growth and does not form colonies when suspended in soft agar, all of which are typical characteristics of non-tumour cells. Due to their mutation of the K-Ras gene, they are considered a pre-tumour cells which represent excellent models of early cancer phenotypes.

Cells were maintained in high glucose Dulbecco's Modified Eagle's Medium (LOBE12614F-Lonza) supplemented with 10% foetal bovine serum (FBS)(ECS0180L-EuroClone), 1% L-Glutamine (ECB3000D) and 1% Penicillin/Streptomycin (ECB3001D). Cells were maintained at 37°C in a humidified atmosphere of 5% CO2 in air.

#### 3.1.2 Cellular treatment

For treatments with each of the different isoforms, a total of $2x10^6$ cells were seeded in p100 dishes. When cells reached 80% of confluence they were treated for 24 hours with: 100 ng/ml of Recombinant human CXCL12-α (catalogue number: 350-NS-050), 100 ng/ml of Recombinant human CXCL12-β (catalogue number: 2716-SD-025) and 100 ng/ml of Recombinant human CXCL12-γ (catalogue number: 6448-SD-025), in FBS-free medium. As control we used cells cultured for 24 hours in FBS-free medium. All proteins were provided by Bio-techne s.r.l. (R&D Systems).

### 3.1.3 Protein extraction and Western Blot Analysis

Protein extraction was performed as follows. After treatments with each CXCL12 isoform, cells were washed twice with cold PBS and then scraped into RIPA lysis buffer containing protease and phosphatase inhibitors. Cells were subsequently centrifuged at 13.000 rpm for 15 minutes at +4°C. The supernatants were used to assess the protein concentration by Bradford assay (#B6916, Sigma Aldrich). The values obtained were compared with a standard curve derived from scalar dilutions of the BSA.

For Western blot analysis, 30 µg of protein samples were boiled for 5 minutes at 95°C, loaded on a 4-12% Tris-Glycine pre-cast gel (Novex # XPO4122BOX Tris-Glycine) [or 4-20% (Novex # XPO4202BOX Tris-Glycine)] and the electrophoretic run was performed using the Tris-Glycine SDS Running Buffer (#LC2675). Using the Mini Blot Module (kit B100A) the proteins were transferred (Tris-Glycine Transfer Buffer, #LC3675) onto a 0.2 µm porose nitrocellulose membrane. The membranes were blocked in TBS-T (Saline Tris Buffer + 0.3% Tween20) containing 5% of BSA (Bovine Serum Albumin, #A7030, Sigma Aldrich) for 1h at RT in shaking. The membranes were then washed three times with TBS-T, the first wash for 10 minutes, the other two for 5 minutes each, and then incubated overnight with the primary antibody at + 4°C. The following morning three washes were performed with TBS-T (1x10'+ 2x5') and then the membranes were incubated 1h at room temperature with the secondary antibody conjugated with HRP. The ECL Super Signal West Pico PLUS (# 34580, Thermo-fisher Scientific) was used as a chemiluminescent substrate that binds to HRP. The chemiluminescent signal was then acquired by development in the darkroom.

Antibodies against GAPDH (#2118L), p-ERK (#4370S), ERK (#4695S), E-cadherin (#3195S), N-cadherin (#4061S), Vimentin (#3932S), Caveolin-1 (#3238S), CD44 (#3578S), p-mTOR (#5536S), m-TOR (#2983S) and Secondary anti-rabbit HRP conjugated (#7074S) were all purchased from Cell Signalling Technology (CST).

### 3.1.4 Wound Healing Assay

"Wound healing" assay was used to detect the alteration of cell motility, an index of change in aggressiveness of the cell that has undergone treatment. Cells were plated in a 6-well plate at a concentration of $50 \times 10^4$ and allowed to form a confluent monolayer overnight. Then the monolayer was scratched with a 100 µL pipette tip, washed 2 times with PBS to remove the floating cells, and maintained in culture medium in the presence or absence of 100 ng/ml of CXCL12-α and CXCL12-β. At time point of 24, 48 and 56 hours later, the wounds were photographed using bright field microscopy at 3 randomly selected sites per well. The actual migration of the cells was analysed according to the original and final wound zone.

### 3.1.5 Soft Agar Assay

Soft Agar Assay was used to determine the effect of the different CXCL12 isoforms on anchorage-independent growth. 5 X 1000 cells were seeded in a six well plate containing 1 mL of complete medium solution and 0.6% of agarose. The same six well were previously overlaid with 1 of complete medium solution and 1% of agarose. Cells were incubated for 18-20 days at 37°C with 5% of $CO_2$. Subsequently, cells were stained with 0.005% crystal violet + 1% Methanol for 1h at room temperature. After many washes with distilled water, the colony formation was evaluated by light microscopy.

### 3.1.6 RNA isolation

RNA was extracted from a total of $2x10^6$ hTERT-HPNE cells treated with the different CXCL12 isoforms. For RNA isolation we used two different purification methods: the TRIzol Reagent and the RNeasy Protect Cell Mini Kit (catalogue number: #74624, Qiagen). The first reagent is composed by phenol, which lyses cells, and guanidine thiocyanate which is a chaotropic agent that inhibits ribonucleases. Through these chemical component the RNA remains in the aqueous phase, while DNA, proteins and lipids concentrate in the organic phase produced by phenol and chloroform. AT the end of extraction, RNA precipitation is carried out with isopropanol.

In the second method, cells are mixed with RNA protect Cell Reagent, which immediately stabilizes the cellular RNA. After RNA stabilization, total RNA is purified using the RNeasy Plus Mini Kit. The cells in RNA protect Cell Reagent are centrifuged, and the resulting cell pellet is lysed and homogenized in Buffer RLT Plus. The lysate is then passed through a gDNA Eliminator spin column, which rapidly and effectively removes genomic DNA. Ethanol is added to the lysate, which is then applied to a RNeasy spin column. After centrifugation, total RNA binds to the membrane of the RNeasy spin column. Contaminants are efficiently washed away, and high-quality total RNA is eluted in 30–50 µl of RNase-free water.

### 3.1.7 Microarray Analysis

All the microarray analysis steps were performed by Cogentech Microarray Unit (Cogentech S.R.L. Benefit Corporation, Via Adamello 16, 20139 Milan, Italy).

The quality of total RNA was first assessed using an Agilent Bioanalyzer 2100 (Agilent Technologies, Palo Alto, CA). Biotin-labelled cDNA targets were synthesized starting from 150 ng of total RNA. Double stranded cDNA synthesis and related cRNA was performed with GeneChip® WT Plus Kit (Affymetrix; Thermo Fisher Scientific, Inc.). Same kit was used to synthesize the sense strand cDNA

before to be fragmented and labelled. All steps of the labelling protocol were performed as suggested by Affymetrix, starting from 5.5 ug of ssDNA. Each eukaryotic GeneChip® probe array contains probe sets for several *B. subtilis* genes that are absent in the samples analysed (lys, phe, thr, and dap). This Poly-A RNA Control Kit contains in vitro synthesized, polyadenylated transcripts for these *B. subtilis* genes that are pre-mixed at high concentrations to allow GeneChip® probe array users to assess the overall success of the assay. Poly-A RNA Controls final concentration in each target are lys 1:100,000, phe 1:50,000, thr 1:25,000 and dap 1:6,667.

Hybridization was performed using the GeneChip® Hybridization, Wash and Stain Kit (Affymetrix; Thermo Fisher Scientific, Inc.). It contains mix for target dilution, DMSO at a final concentration of 7% and pre-mixed biotin-labelled control oligo B2 and bioB, bioC, bioD and cre controls (Affymetrix cat #900299) at a final concentration of 50 pM, 1.5 pM, 5 pM, 25 pM and 100 pM, respectively. Fragmented and labelled sscDNA were diluted in hybridization buffer at a concentration of 23 ng/ul for a 2.3 ug total and denatured at 99 °C for 5 minutes incubated at 45 °C for 5 minutes and centrifuged at maximum speed for 1 minute prior to introduction into the GeneChip® cartridge. A single GeneChip® Clariom S was then hybridized with each biotin-labelled sense target. Hybridizations were performed for 16 h at 45 °C in a rotisserie oven (60 RPM). GeneChip® cartridges were washed and stained with GeneChip® Hybridization, Wash and Stain Kit in the Affymetrix Fluidics Station 450 following the FS450_0007 standard protocol, including the following steps: (1) (wash) 10 cycles of 2 mixes/cycle with Wash Buffer A at 30 °C; (2) (wash) 6 cycles of 15 mixes/cycle with Wash Buffer B at 50 °C; (3) stain of the probe array for 5 min in SAPE solution at 35 °C; (4) (wash) 10 cycles of 4 mixes/cycle with Wash Buffer A at 30 °C; (5) stain of the probe array for 5 min in antibody solution at 35 °C; (6) stain of the probe array for 5 min in SAPE solution at 35 °C; (7) (final wash) 15 cycles of 4 mixes/cycle with Wash Buffer A at 35 °C; (8) fill the probe array with Array Holding buffer.

GeneChip arrays were scanned using an Affymetrix GeneChip® Scanner 3000 7G using default parameters. Affymetrix GeneChip® Command Console software (AGCC) was used to acquire GeneChip® images and generate .DAT and .CEL files, which were used for subsequent analysis with proprietary software.

#### 3.1.7.1 Normalization and Batch effect

For statistical analysis we used R, a programming language commonly used for statistical computing/calculation in the scientific field. All data obtained from microarrays scanning, both treated and the controls, were subjected to background correction and normalization procedures. With the first method the bias, or the "background noise", which could be generated by incorrect pairing between the probe and target or by errors during the signal detection procedure, was significantly

reduced. The second method, instead, serves to make the variation of the intensities and the ratio of the sample-control intensities independent of their absolute value, allowing the comparison between arrays. RMA (Robust Multiarray Analysis) is the algorithm chosen for this processing. The data is reported according to the log2 function.

In this work we have chosen to use the ComBat algorithm to remove the "batch effect" due to several experimental variables, such as: the use of different RNA extraction kits, the different environmental conditions in which the experiments are carried out, the different levels of experience of the operators and the use of different array platforms. Thanks to this correction it was possible to eliminate those small variations, present among the results, which had not been eliminated during the normalization phase.

This algorithm, within a data set of genes, detects systematically repeating errors and corrects them based on the hypothesis that the phenomena that resulting in the batch effect frequently influence numerous different genes in an analogous manner. Hence, ComBat, identifies the parameters which represent the batch effects among the genes considered to apply them subsequently to the whole dataset correcting the data bias from the batch effect [49].

#### 3.1.7.2 Analysis of differentially expressed genes

Of the Bioconductor package, the Limma algorithm, run in R, was used to highlight the differentially expressed genes between the treated samples and the control. Limma uses a linear mathematical model and attributes to each gene a coefficient expressed in a logarithmic function that takes into account the distribution of the other genes in the dataset. In order to have statistically significant values, the False Discovery Rate (FDR) was used to correct the data obtained. Only the coefficients of the genes with a corrected P value (p-adj) of less than 0.05 have been taken into consideration.

#### 3.1.7.3 Functional Enrichment

In order to correlate the differentially expressed genes to the pathways involved, functional enrichment was performed. The Enrichr platform was used for this procedure (https://amp.pharm.mssm.edu/Enrichr/). This database contains 153 different libraries, each of which contains all the genes of the main model organisms. Below are the names of the libraries used: WikiPathway 2019, Kegg 2019 Human and GO Biological Process 2018. Thanks to these libraries, it is possible to calculate the expected value, that is the probability that a given gene belongs to a certain pathway. After having inserted the list of our differentially expressed genes, the database, by algorithm, estimates the probability of obtaining a result as close as possible to the expected value. Once this process has been completed, each pathway obtained from the server search is associated with a p value which indicates the statistical significance relative to each pathway. The values of p <0.05 are considered acceptable. In our study, only genes whose expression was 1. 5 times higher

(upregulated) or 1. 5 times lower (downregulated) than the control were subjected to functional enrichment (in terms of fold change it corresponds to: FC<;0. 67 or FC>1. 5).

### 3.1.8 RT-qPCR

For the Real-Time PCR, we synthesized cDNA using a Reverse Transcription System (#601-005, HyperScript First Strand Synthesis Kit, GeneAll). We used SYBR Green (#RR420A, TB Green Premix EX Taq, Takara) on an StepOnePlus™ Real-Time PCR System (Thermo Fisher Scientific). The primer sequences were as follows: EZH2 Fw 5'-CCCTGACCTCTGTCTTACTTGTGGA-3', Rev 5'-ACGTCAGATGGTGCCAGCAATA-3', PTPRB Fw 5'-ACAACACCACATACGGATGTAAC-3', Rev 5'-CCTAGCAGGAGGTAAAGGATCT-3', DPP4 Fw 5'-CTCCAGAAGACAACCTTGACCATTACAGAA-3', Rev 5'-TCATCATCATCTTGACAGTGCAGTTTTGAG-3' and GAPDH Fw 5'-TGCACCACCAACTGCTTA-3', 5'-Rev GGATGCAGGGATGATGTTC-3'. The temperature conditions for real-time PCR assays were as follows: stage 1, 95 °C for 30s; stage 2 (X40), 95 °C for 5s and 60°C for 34s (varies based on primer probes), stage three 95° for 15s, 60° for 1m and 95° for 15s. Threshold cycle (CT) values of gene of interest were normalized against CT values for GAPDH, and a relative fold change in expression against a reference sample was calculated by the 2-ΔΔCt method.

## 3.2 EXOSOMES

### 3.2.1 ELISA Assay

During my master thesis, the ELISA technique was developed and optimized. We have chosen to use this method because it is quantitative and highly specific, thanks to the use of antibodies. Briefly, the ELISA consists of a “sandwich-type” assay, in which capture antibodies are immobilized on modified surface microplates; subsequently, all the surfaces on which the antibody is not bound are blocked, the sample is incubated overnight, a primary and a secondary antibody are used to recognize the bound antigen and finally the signal is revealed through a colorimetric reaction.

For the ELISA test, transparent 96-well plates with high protein binding capacity (Nunc MaxiSorp ™, Thermo Fisher Scientific) were used. In each well the anti-Rab5b antibody, dissolved in a sodium carbonate buffer solution, was incubated overnight at + 4°C. Subsequently, for each well, 3 washes were performed with a buffer solution of 1X PBS and 0.1% Tween 20 (PBST). The blocking procedure was performed for 90 minutes at room temperature and in shaking, filling the wells with PBS + 1% of BSA (Bovine Serum Albumin). After additional 3 washes with PBST, each patients’ plasma was incubated initially for 2 hours at 37°C and then overnight at + 4°C. The following day, after 3XPBST washes, the primary antibody was added to each well and allowed to incubate for 3

hours at room temperature. Following another 3 washes, the secondary antibody was added and incubated for 45 minutes at room temperature. After washing, Streptavidin Poly-HRP was incubated for 45 minutes at room temperature.

The dilution buffer used for all the antibodies is PBS with 300 mM NaCl, 0.05% Tween 20, 0.5% BSA. After the last incubation period, the 1-Step ™ Ultra TMB-ELISA (Thermo Fisher Scientific) substrate solution was added for 20 minutes at room temperature, in shaking, and the reaction was stopped with 2M Sulfuric Acid.

Optical densities were recorded at 450 nm using the Micrisklate FC Multiskan photometer (Thermo Fisher Scientific). The Wellwash ™ Versa Microplate Washer (Thermo Fisher Scientific) was used to perform the microplate washes to ensure intra-assay repeatability. Incubations have also been conducted in conditions of darkness.

To regulate our protocol, we used freeze-dried exosomes from the plasma of healthy donors (cat HBM-PEP-100/4, HansaBioMed Life Sciences Ltd, Tallin, Estonia). For each plate and for each type of antibody the absorbance value of the sample (signal) was divided by the absorbance of the blank (noise) to obtain a normalized value. Vacuum is obtained by testing PBS instead of plasma.

### 3.2.2 Antibodies used

To isolate exosomes using the ELISA technique, the following mouse monoclonal primary antibodies were used:

- anti-human CD151 (#271216) and Alix (#53540) were purchased from Santa Cruz Biotechnology.
- anti-human TSPAN8 (# WH0007103M2) was purchased from Sigma-Aldrich, Italy;
- anti-human CD9 (# 555370), CD81 (#555675), CD24 (# 555426), Caveolin-1 (# 610407) and Fibronectin (# 610077). They were purchased from BD Biosciences, USA;
- anti-human CD133 (# MAB11331), PD-L1(# MAB1561), CXCR4 (# MAB172), EpCAM (#MAB9601), Integrin α6 (# MAB1350), Integrin β4 (# MAB4060), CD44s (# MAB7045) and CD44v6 (# BBA13) was purchased from R&D System, Minneapolis, USA.

As capture antibody, Rab5b polyclonal rabbit antibody anti-human (# HBM-RAB5-PR1) (Hansa BioMed Life Sciences Ltd, Santa Cruz Biotechnology) was used.

Goat anti-mouse biotin conjugated antibody (#A16076) (Thermo Fisher Scientific) was used as secondary antibody. Streptavidin Poly-HRP (#21140) (Thermo Fisher Scientific) is used to amplify the signal.

### 3.2.3 Experimental condition of patients and blood samples

The Medical Oncology Unit of Ancona Hospital has enrolled patients for the present study.

Nineteen individuals with pancreatic ductal adenocarcinoma were enrolled, all candidates to receive chemotherapy with the following drugs: Gemcitabine + Nab-Paclitaxel, FOLFIRINOX or mono-chemotherapy with Gemcitabine. To assess the response of each patient to radiological treatments, the RECIST criteria (Response Evaluation Criteria in Solid Tumours) was used, a series of guidelines applied to define the status of the tumour following pharmacological treatment. This assessment was carried out 12 weeks after the first treatment and then every three months. The data collected allowed us to define, for each patient, the two very important criteria:

- Progression-Free Survival (PFS): it is the time elapsed between the first cycle of chemotherapy and the first radiological progression;
- Overall Survival (OS): is the time elapsed between the first cycle of chemotherapy and the patients' death.

For our study, blood samples were collected at time point "T0", antecedent to the chemotherapy treatment, and at time point T3, which instead corresponds to the period of 3 months after chemotherapy treatment.

Samples were processed as follows: EDTA-plasma was separated from blood cells by centrifugation at 1100 g for 20 minutes at room temperature (RT). A further centrifugation at 10,000g at +4°C for 7 minutes, allowed the micro-vesicles elimination from the supernatant. Once the sample was processed the plasma obtained from each patient was stored at -80 ° C until the use.

# 4. RESULTS

## 4.1 CXCL12

### 4.1.1 Expression of mesenchymal and staminal markers in h-TERT HPNE cell lines following CXCL12 isoforms stimulation

The effect of the two commercially available isoforms of CXCL12, the isoform-α and the isoform-β, has been evaluated by western blot analysis, in the non-cancer h-TERT HPNE cell line. By exposing cells for 24 hours to treatment with one or the other isoform, a notable increase in mesenchymal markers has been observed, such as Vimentin and N-cadherin. In particular, the treatments with the α-isoform, compared to the β-isoform, induced a greater over-expression of Vimentin (Ratio: 1,37 and 0,81). Vimentin, the main protein constituent of the intermediate filaments, is produced at the level of normal endothelial and mesenchymal cells [50]. It is known that in normal physiological processes it plays an important role in the processes of adhesion, migration and cellular communication. In fact, in tumours, if its expression is altered, this protein is considered an important marker of mesenchymality in the epithelial-mesenchymal transition (EMT) [51, 52]. The N-Cadherin mesenchymal marker is over-expressed in cells treated with both α and β isoforms (ratio: 0.50 and 0.39, respectively), compared to the control one (Ratio: 0,18).

Furthermore, when h-TERT HPNE cells have been treated with 100ng/ml of CXCL12 isoforms, they showed a low overexpression of CD44 staminal marker. In particular, the β-isoform induced a greater expression of this protein, respect the α-isoform (Ratio: 1,41 and 1,39, respectively). This transmembrane protein is implicated in numerous cellular mechanisms like cell growth, adhesion, proliferation and migration. The overexpression of CD44 and its isoforms is associated with poor PDAC prognosis [53-55].

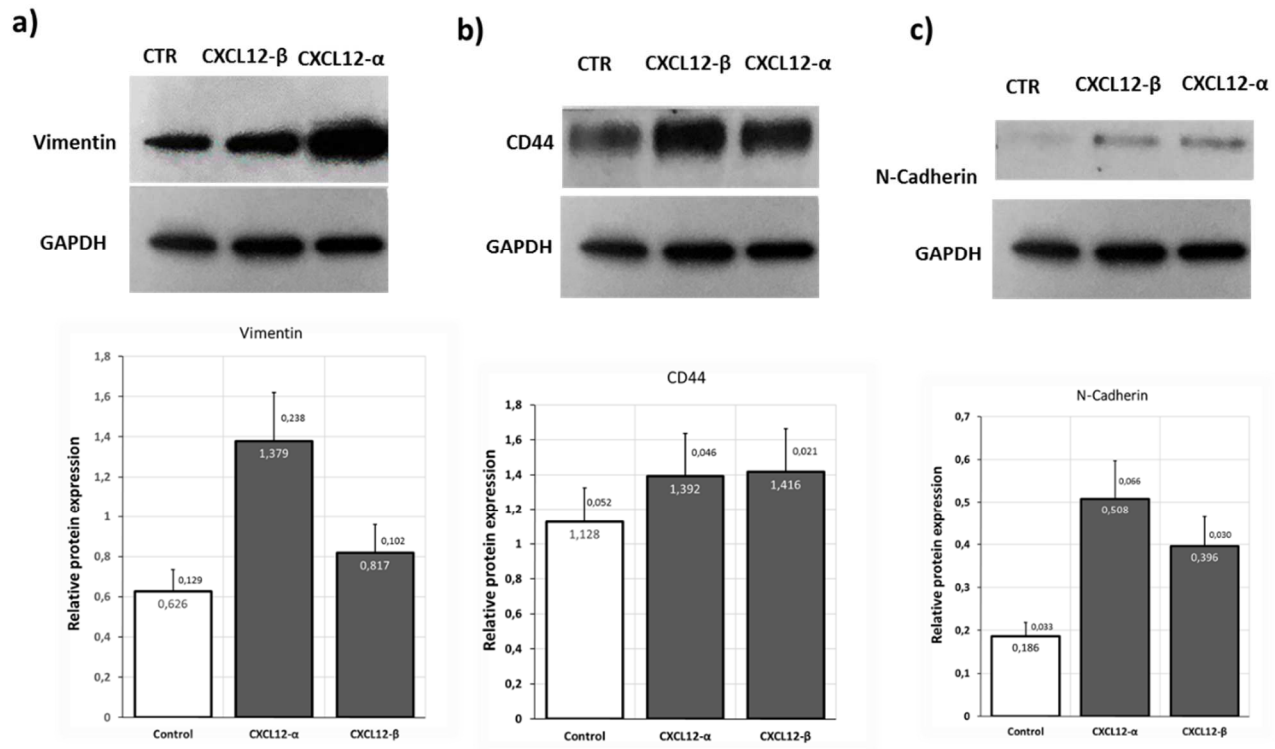


***Figure 3.*** *Western blot Analysis of h-Tert HPNE cells treated for 24 hours with 100 ng/ml of CXCL12-α and CXCL12-β isoforms. The signal intensity of each protein expression was obtained by ImageJ software. a) cells treated with CXCL12-α shown a greater expression of Vimentin; b) cells treated with CXCL12-β express more CD44 than cells treated with CXCL12-α; c) N-cadherin expression is higher following treatment with CXCL12-α.*

### 4.1.2 CXCL12 treatment leads to mTOR and ERK activation

Treating h-Tert HPNE cells for 24 h with each isoform of CXCL12, α and β, at the concentration of 100ng / ml, we noticed an increase in mTOR and ERK phosphorylation. Compared to the control (Ratio: 0.65), both treatments with the α and β isoforms induced an increase in mTOR phosphorylation (ratio of 0,94 and 0,92 respectively). There are no major differences between the two isoforms, α and β, which almost equally induce phosphorylation of mTOR.

Also for ERK, compared to the control (Ratio: 0,56), both α and β isoforms induced an increase in phosphorylation (ratio of 0,89 and 1,15, respectively). Compared to CXCL12-α, the β-isoform induced greater phosphorylation of ERK, about 30% more.

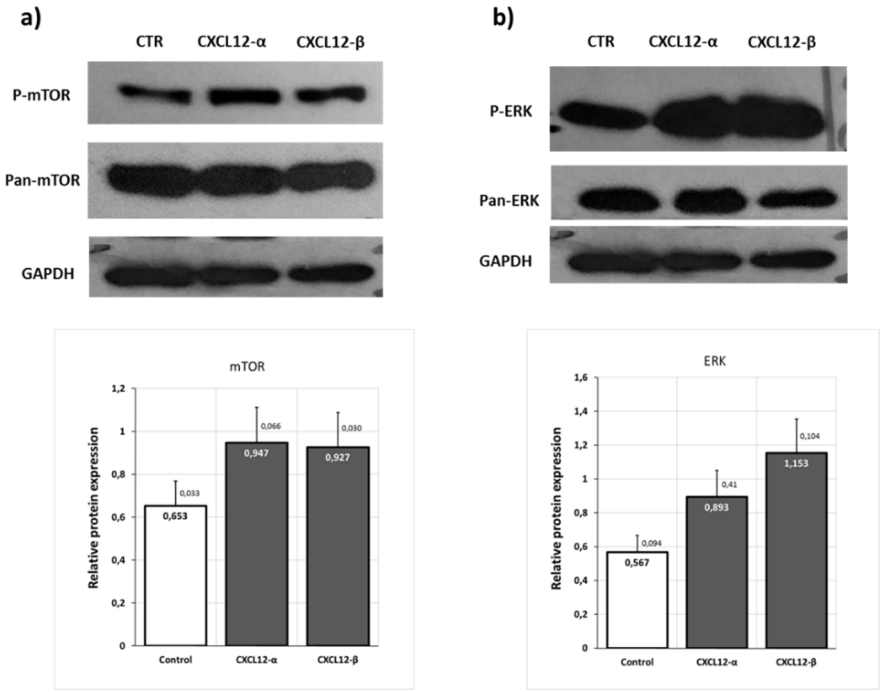


***Figure 4.*** *Western blot Analysis of h-Tert HPNE cells treated for 24 hours with 100 ng/ml of CXCL12-α and CXCL12-β isoforms. The signal intensity of each protein expression was obtained by ImageJ software. a) CXCL12-α and CXCL12-β isoforms induce in the same way an increase in mTOR phosphorylation; b) CXCL12-β more than CXCL12-α induces a ERK phosphorylation.*

### 4.1.3 CXCL12-α induces a migration increase

To assess the ability of cell migration, following treatment with the α and the β isoforms, the Wound Healing Assay was performed. Comparing the rate of invasion between untreated cells and those treated with each isoform, I have observed that α-isoform induced an increase in cell migration rate. This increase, also correlated with the protein expression data mentioned above, shows that the α-isoform treatment leads to a more aggressive cellular phenotype.

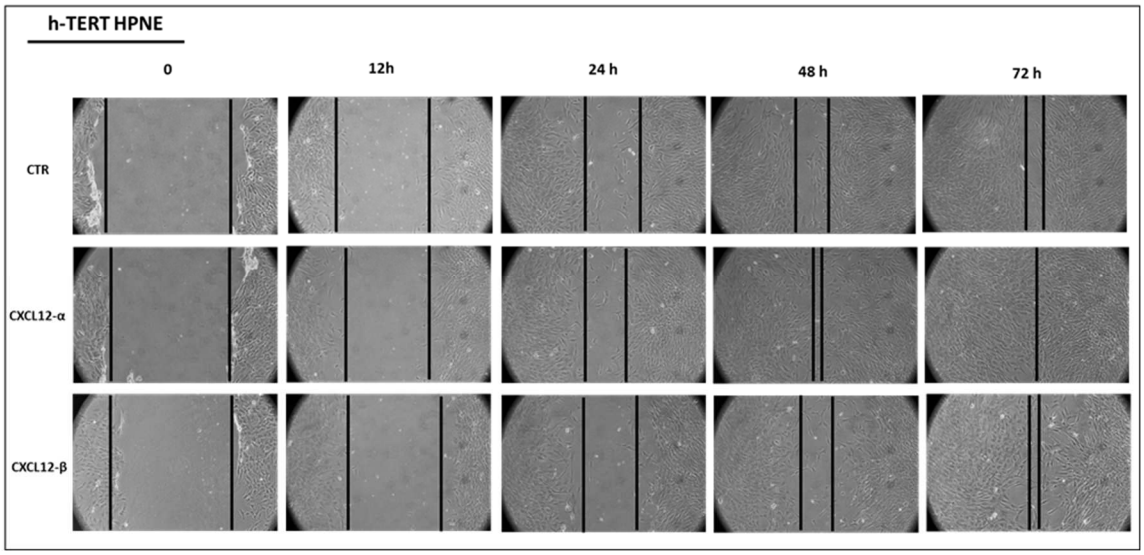


***Figure 5.*** *Wound Healing Assay of h-Tert HPNE cells.*

### 4.1.4 Soft-agar Assay

The anchorage independent growth of h-Tert HPNE treated with CXCL12 isoforms, was determined in a soft agar assay. From a first analysis, the cells treated separately for 24h with 100ng/ml of each of the two isoforms, do not form colonies in the semi-solid layer of agar. The brief treatment with CXCL12-α and CXCL12-β was therefore not sufficient to induce a neoplastic transformation in our hTERT-HPNE cells. It will certainly be interesting to evaluate this transformation following a constant and repeated administration, for at least 7-10 days, with each of others isoforms.

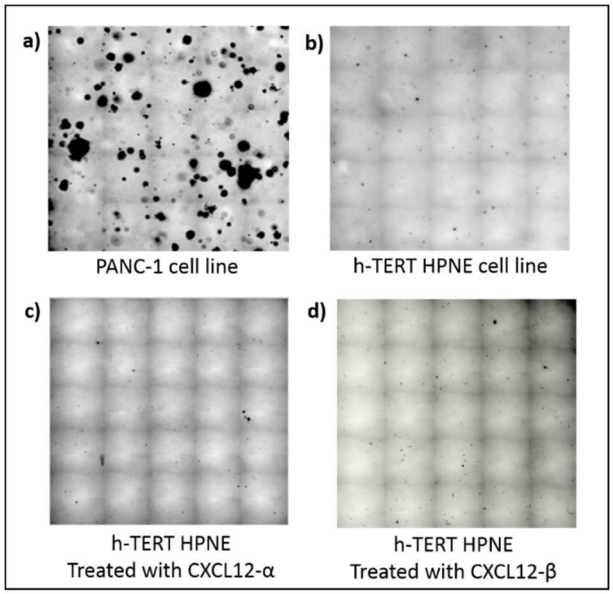


***Figure 6.*** *The effect of CXCL12 isoforms on soft-agar colony formation in h-Tert HPNE cell line. a) Soft agar assay of Panc-1 cell line was used as positive control. b) h-TERT HPNE cell line was used as negative control. c-d) h-TERT HPNE cell line was treated with CXCL12-α and CXCL12-β respectively.*

### 4.1.5 Microarray Analysis

The RNA extracted from the treated samples and from the control sample was sent to an external company to perform the Microarray analysis. In order to allow comparison between arrays, making both the intensity variation (deriving from each spot) and the ratio of the treated-control intensities independent of the absolute value, the data obtained by scanning the microarray were subjected to normalization.

From a first analysis, as shown in figure 1, it emerges that the cluster reported in blue, corresponding to the samples treated with CXCL12-γ, is distanced and appear quite distinct from the other groups. This phenomenon can be explained by the use of a different kit with which the RNA of the samples treated with γ (RNeasy Protect Cell Mini Kit) was extracted, compared to the kit used for the treated and control samples (Trizol). In order to remove any different experimental conditions (Batch

effects), we used the ComBat algorithm. Through this program the data of the CXCL12- γ treated sample have been standardized to those of the other samples, so as to be able to make a comparison.

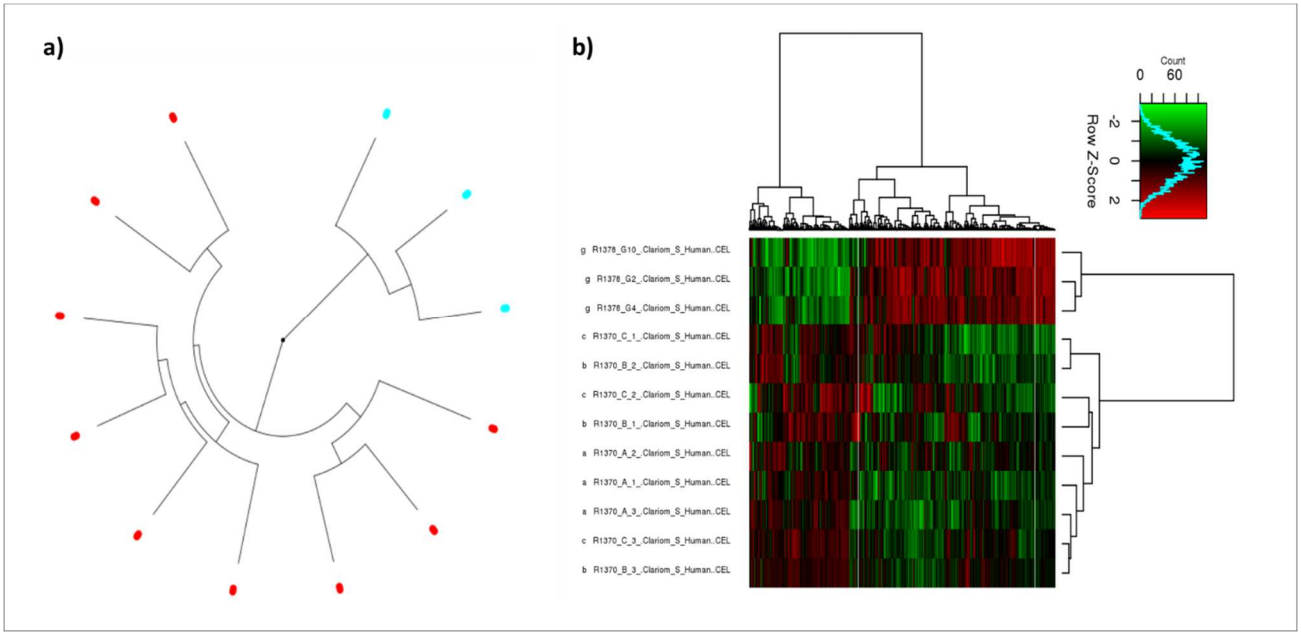


***Figure 7.*** *Clustering analysis before using ComBat. a) Circular dendrogram before batch effect correction. Samples treated with CXCL12-γ (blue) form a very distinct group respect to control, CXCL12-α e CXCL12-β samples (red). b) Heatmap showing gene expression profile of samples before batch effect correction. Samples treated with CXCL12-γ (green) form a very distinct group respect to control, CXCL12-α e CXCL12-β samples (red).*

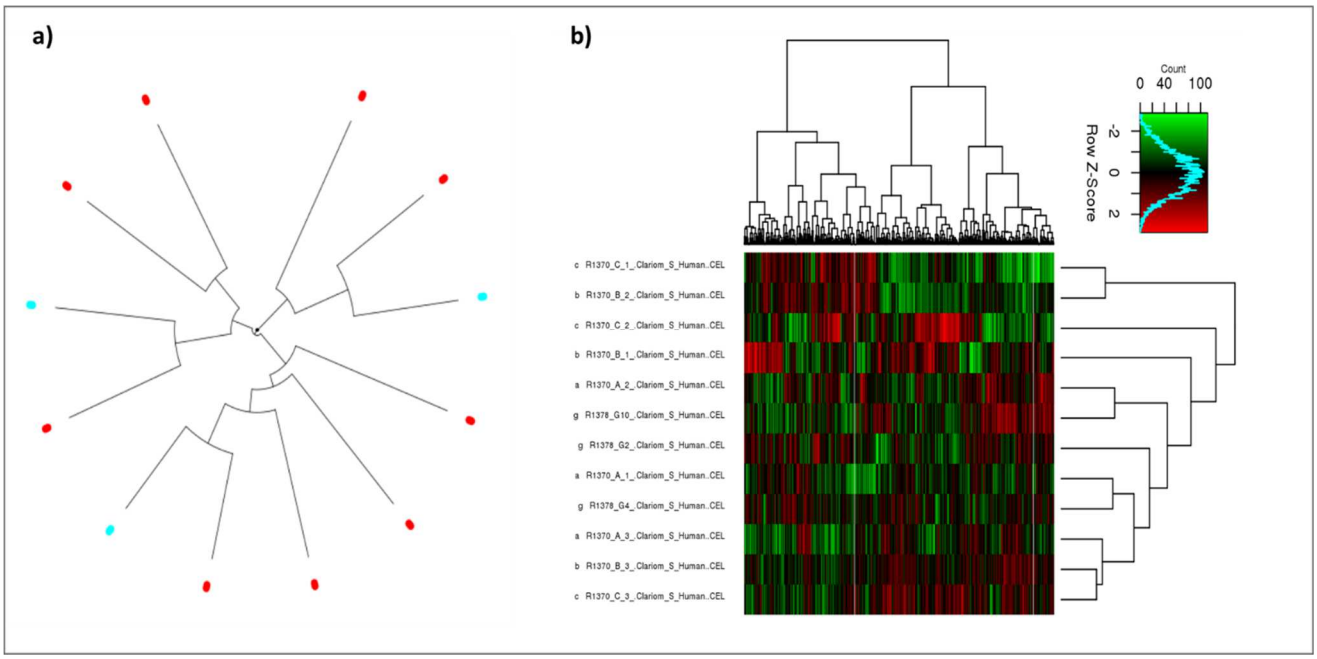


***Figure 8.*** *Clustering analysis after using ComBat. a) As shown in the circular dendrogram, after batch effect correction, samples treated with CXCL12-γ are equally distributed and can be compared with other samples. b) Heatmap showing gene expression profile of samples after batch effect correction. Samples treated with CXCL12-γ (green) are more evenly distributed respect to control, CXCL12-α e CXCL12-β samples (red).*

#### 4.1.5.1 Variation of gene expression profile

Through the Limma algorithm was performed the variation of gene expression, deriving from the comparison between each treated sample and the control. As shown in table 1, after correcting the p-values for the False Discovery Rate (FDR), they were found to be differentially expressed (Fold Change (FC) < - 1.5 or > 1.5 with p-value adj < 0.05) in 48 genes for the sample treated with the CXCL12-α isoform, 48 genes for the sample treated with the CXCL12-β isoform and 31 genes for the sample treated with the CXCL12-γ isoform.

***Table 1.*** *Comparison of main differentially expressed genes in samples treated with CXCL12-α, CXCL12-β and CXCL12-γ, respect to the control sample. The values highlighted are those that had a fold change value <-1.5 or > 1.5, with p-adj <0.05.*

| Gene Name | Treated with CXCL12-α | Treated with CXCL12-β | Treated with CXCL12-γ |
|---|---|---|---|
| **ACSS2** | **-1,66** | **-1,51** | **-1,64** |
| **AKAIN1** | **1,51** | **1,57** | **1,53** |
| **ANK2** | **-1,70** | **-1,53** | **-1,59** |
| **APOBEC1** | **-1,64** | -1,33 | -1,45 |
| **ATP6V1G3** | **1,58** | 1,30 | 1,37 |
| **AZI2** | 1,33 | **1,59** | **1,65** |
| **BMP7** | **1,56** | 1,22 | 1,32 |
| **C9orf40** | **1,52** | **1,68** | **1,56** |
| **CACNA1A** | **1,53** | 1,02 | 1,20 |
| **CARMIL1** | **1,74** | -1,04 | 1,27 |
| **CCR1** | **1,63** | **1,52** | **1,52** |
| **CEP295** | 1,22 | **1,59** | 1,36 |
| **CNBD2** | **-1,57** | -1,49 | -1,35 |
| **CNGB1** | **1,83** | 1,33 | **1,50** |
| **DEFB106B** | -1,21 | **-1,62** | -1,39 |
| **DIO1** | -1,48 | **-1,52** | **-1,50** |
| **DOCK10** | **-2,01** | **-1,73** | **-1,91** |
| **DPP4** | 1,15 | **1,68** | 1,42 |
| **DUXA** | **-1,52** | -1,28 | -1,34 |
| **ELFN1** | **-1,64** | -1,26 | -1,45 |
| **ENTPD5** | 1,18 | **1,61** | 1,36 |
| **ERP27** | 1,00 | **-1,57** | -1,20 |
| **FEM1C** | **1,56** | **2,10** | **1,86** |

| | | | |
|---|---|---|---|
| **FMN1** | **-1,54** | 1,02 | -1,17 |
| **GMNC** | **-1,77** | -1,38 | **-1,66** |
| **GNAQ** | **-1,62** | -1,43 | **-1,55** |
| **GPCPD1** | **-1,53** | 1,00 | -1,22 |
| **HMBS** | **-1,54** | **-1,53** | **-1,53** |
| **IFNG** | 1,04 | **1,51** | 1,22 |
| **IFNGR2** | -1,40 | **-1,67** | **-1,51** |
| **INAVA** | **-1,53** | -1,46 | -1,43 |
| **JAK2** | -1,07 | **-1,65** | -1,26 |
| **KIF25** | **1,57** | **1,86** | **1,64** |
| **LMNB2** | -1,49 | **-1,53** | **-1,53** |
| **LOC339862** | **1,71** | 1,27 | 1,41 |
| **MICALCL** | **1,59** | 1,10 | 1,29 |
| **MMRN1** | **1,79** | 1,47 | **1,60** |
| **MSLN** | -1,13 | **-1,59** | -1,37 |
| **MTA3** | **1,68** | 1,23 | 1,39 |
| **NDUFA3** | **-1,53** | **-1,51** | **-1,53** |
| **NEUROG2** | **1,94** | 1,31 | **1,53** |
| **NLK** | **-1,52** | -1,22 | -1,34 |
| **NPFFR2** | 1,47 | 1,62 | 1,47 |
| **OR6A2** | **-1,79** | **-1,66** | **-1,72** |
| **OR9G4** | -1,18 | **-1,50** | -1,33 |
| **P3H2** | **-1,52** | -1,27 | -1,33 |
| **PAGE3** | -1,42 | **-1,60** | -1,48 |
| **PEX7** | **1,50** | 1,28 | 1,37 |
| **POGZ** | **-1,60** | **-1,59** | **-1,57** |
| **PTPRB** | **-1,58** | **-1,57** | -1,52 |
| **PUS7** | 1,32 | **1,66** | 1,43 |
| **QSOX2** | 1,36 | **1,58** | 1,43 |
| **RAB3A** | -1,27 | -1,62 | -1,43 |
| **RHCG** | -1,30 | **-1,51** | -1,37 |
| **RHEBL1** | -1,33 | **1,53** | 1,03 |
| **RNF112** | **1,62** | 1,16 | 1,34 |
| **SCN3A** | -1,24 | **-1,74** | **-1,52** |
| **SCRIB** | -1,20 | **-1,63** | -1,37 |
| **SERPINA6** | **1,64** | 1,26 | 1,44 |
| **SFRP5** | **1,62** | **1,59** | **1,55** |

| | | | |
|---|---|---|---|
| **SFTPC** | -1,39 | **-1,58** | -1,46 |
| **SH2D5** | **1,57** | 1,32 | 1,33 |
| **SIPA1L2** | -1,43 | **-1,67** | **-1,62** |
| **SLC17A1** | -1,38 | **-1,50** | -1,41 |
| **SPACA6** | **-1,66** | **-1,58** | **-1,64** |
| **SPDYE4** | **1,67** | 1,17 | 1,32 |
| **STMN2** | **-1,73** | -1,44 | **-1,56** |
| **SYT9** | **1,55** | 1,13 | 1,40 |
| **TEX46** | **-1,53** | -1,15 | -1,32 |
| **TMPRSS13** | -1,12 | **-1,56** | -1,26 |
| **WDR12** | **1,51** | **1,57** | **1,55** |
| **WNT2B** | -1,44 | **-1,67** | **-1,59** |
| **ZBED6CL** | 1,32 | **1,55** | 1,39 |
| **ZBED9** | **-1,67** | **-1,71** | **-1,71** |
| **ZNF124** | **1,57** | **1,65** | **1,62** |
| **ZNF502** | **-1,62** | **-1,70** | **-1,73** |

Treatments with the three different CXCL12 isoforms (α, β and γ) induce an alteration in each expression profile of reported gene. Often, up- or down-regulation is evident in all treated samples, where at least one has an FC value lower than -1.5 or greater at +1.5 (BMP7, PTPRB, ANK2, NEUROG2, MSLN). It also happens that only one of treated samples has a de-regulation, for example: SCRIB gene is de-regulated only in samples treated with CXCL12- β, while SERPINA6 gene is de-regulated only for CXCL12-α treated ones.

Regarding to the RHEBL1 gene, it has a different expression profile depending on the treatment to which the sample has been exposed. In fact, by treating sample with α-isoform, the RHEBL1 gene is up-regulated, while the treatment with CXCL12-β caused its down-regulation. When the sample was treated with CXCL12-γ, the expression of this gene remained unchanged, comparable to control sample.

#### 4.1.5.2 Main differentially expressed genes in the sample treated with CXCL12-α

**Table 2.** Main differentially expressed genes in samples treated with CXCL12-α.

| **Treated CXCL12-α** |
|---|

| Symbol | Gene Name | Fold Change |
|---|---|---|
| **DOCK10** | dedicator of cytokinesis 10 | -2,01 |
| **OR6A2** | olfactory receptor family 6 subfamily A member 2 | -1,79 |
| **GMNC** | geminin coiled-coil domain containing | -1,77 |
| **STMN2** | stathmin 2 | -1,73 |
| **ANK2** | ankyrin 2 | -1,70 |
| **LOC339862** | uncharacterized LOC339862 | 1,71 |
| **CARMIL1** | capping protein regulator and myosin 1 linker 1 | 1,74 |
| **MMRN1** | multimerin 1 | 1,79 |
| **CNGB1** | cyclic nucleotide gated channel beta 1 | 1,83 |
| **NEUROG2** | neurogenin 2 | 1,94 |

The analysis of the differentially expressed genes showed that following treatment with the α-isoform, cells show a de-regulation of the ANK2 and STMN2 genes; both genes showed a greater alteration of expression compared to the control sample. The STMN2 gene transcribes for Statmina2, a protein that takes part in microtubules stabilization processes and is highly expressed in central nervous system cells. This protein has been proposed as a tumour marker since it is highly expressed in hepatic cancer cells [56]. Instead, from our Microarray analysis, following the treatment with CXCL12-α, there is a decrease in STMN-2 expression, also confirmed in samples treated both with the β-isoform and the γ-isoform, but with CF values lower than those observed for the sample treated with CXCL12-α.

Concerning the ANK-2 gene, overexpression has been described in relation to ductal adenocarcinoma and it is known that the invasive capacity of pancreatic cancer cells can also be attenuated by inhibiting the expression of this gene [57]. This gene, in fact, transcribes for a protein, Ankyrina B, involved in processes like cell motility and proliferation. In our analysis, a down-regulation of the ANK-2 gene is observed upon treatment with the α-isoform. This de-regulation can be also found in samples treated with CXCL12-β and CXCL12-γ.

#### 4.1.5.3 Main differentially expressed genes in the sample treated with CXCL12- β

**Table 3.** Main differentially expressed genes in samples treated with CXCL12-β.

| **Treated CXCL12-β** | | |
|---|---|---|
| **Symbol** | **Nome Gene** | **Fold Change** |
| **ZNF502** | zinc finger protein 502 | -1,70 |

| | | |
|---|---|---|
| **SCN3A** | sodium voltage-gated channel alpha subunit 3 | -1,74 |
| **DOCK10** | dedicator of cytokinesis 10 | -1,73 |
| **ZBED9** | zinc finger BED-type containing 9 | -1,71 |
| **WNT2B** | Wnt family member 2B | -1,67 |
| **PUS7** | pseudouridine synthase 7 like | 1,66 |
| **DPP4** | dipeptidyl peptidase 4 | 1,68 |
| **C9orf40** | chromosome 9 open reading frame 40 | 1,68 |
| **KIF25** | kinesin family member 25 | 1,86 |
| **FEM1C** | fem-1 homolog C | 2,10 |

Among differentially expressed genes in cells treated with CXCL12-β, we distinguish DPP4 and WNT2B. The latter is an essential gene in the Wnt β-catenin pathway and in physiological conditions it is related to the processes of proliferation, embryonic development and tissue homeostasis, while in pathological ones it is frequently alterated in the cancer onset. Treatment with the CXCL12-β isoform in the H-Tert HPNE cells induces a de-regulation of the WNT2B gene. This gene is also downregulated in the γ-isoform, while its de-regulation is not significant in α-isoform.

DPP4 instead, is a gene that encodes for the serine protease dipeptidilpeptidase-4 present on the cell surface and it is able to cut the N-terminal protein portion with consequent alteration of protein functional activity. Treatment with the β-isoform induces an up-regulation of DPP4 with consequent post-translational modifications to CXCL12 and consequent chemokine inactivation which, however, still remains able to binding the CXCR4 receptor [14]. In the other two treatments, with the α isoform and the γ isoform, this over-expression of the DPP4 gene is not observed.

#### 4.1.5.4 Main differentially expressed genes in the sample treated with CXCL12-γ

**Table 4.** Main differentially expressed genes in samples treated with CXCL12-γ.

| **Treated CXCL12-γ** | | |
|---|---|---|
| **Symbol** | **Nome Gene** | **Fold Change** |
| **DOCK10** | dedicator of cytokinesis 10 | -1,91 |
| **ZNF502** | zinc finger protein 502 | -1,73 |
| **OR6A2** | olfactory receptor family 6 subfamily A member 2 | -1,72 |
| **ZBED9** | zinc finger BED-type containing 9 | -1,71 |
| **GMNC** | geminin coiled-coil domain containing | -1,66 |
| **MMRN1** | multimerin 1 | 1,60 |

| | | |
|---|---|---|
| **ZNF124** | zinc finger protein 124 | 1,62 |
| **KIF25** | kinesin family member 25 | 1,64 |
| **AZI2** | 5-azacytidine induced 2 | 1,65 |
| **FEM1C** | fem-1 homolog C | 1,86 |

Likewise, samples treated with CXCL12-γ showed alteration of several genes, including the AZI2 gene (5-azacytidine-induced protein2) which is related to the NFK-B transcription factor activation. This factor is responsible for the transcription of numerous genes related to processes such as cell proliferation, survival, oncogenesis, as well as inflammatory and immune response. From the microarray data it has been found that CXCL12- γ induces an over-expression of AZI2 gene, such significance has been also found in the cells treated with CXCL12-β, but not in those treated with CXCL12-α.

#### 4.1.5.5 Pathways involved: functional enrichment

In order to identify the alteration of those pathways that were statistically significant, following treatment with CXCL12-α, CXCL12-β and CXCL12-γ isoforms (p-value < 0.05), we used the method of functional enrichment. For this analysis the following Enrichr database libraries have been consulted: GO Biological Process 2018, WikiPathway 2019 and Kegg 2019 Human. The identified pathways, divided by each isoform treatments, are listed in the following tables.

***Table 5**. Alterated pathways in cells treated with CXCL12-α isoform.*

| **LIBRARY** | **STATISTICALLY SIGNIFICANT PATHWAYS IN SAMPLES TREATED WITH CXCL12-α** | **p-value** |
|---|---|---|
| **GO biological Process 2018** | Negative regulation of mitotic nuclear division | 0.00025 |
| | Regulation of catenin import into nucleus | 0.00104 |
| | Calcium ion transport | 0.00292 |
| | Positive regulation of calcium ion transport | 0.00301 |
| | Regulation of bone mineralization | 0.00667 |
| | Regulation of calcium ion transport | 0.00718 |
| | Positive regulation of cell projection organization | 0.01034 |
| | Negative regulation of muscle cell apoptotic process | 0.01668 |
| | Regulation of cellular response to oxidative stress | 0.01668 |
| | Negative regulation of vasculature development | 0.01668 |
| | Mitotic sister chromatid segregation | 0.01696 |

| | | |
|---|---|---|
| | Positive regulation of supramolecular fiber organization | 0.01774 |
| | Calcium ion homeostasis | 0.01894 |
| | Cellular phosphate ion homeostasis | 0.01904 |
| | Leukocyte aggregation | 0.01904 |
| | Cellular lipid biosynthetic process | 0.01904 |
| | Marginal zone B cell differentiation | 0.01904 |
| | Divalent metal ion transport | 0.01934 |
| | Actin filament network formation | 0.02140 |
| | Kinetochore assembly | 0.02140 |
| | Cell junction maintenance | 0.02140 |
| | Cellular metal ion homeostasis | 0.02272 |
| | Positive regulation of neuron projection development | 0.02316 |
| | Mature B cell differentiation involved in immune response | 0.02375 |
| | Regulation of methylation-dependent chromatin silencing | 0.02375 |
| | Regulation of sequestering of calcium ion | 0.02375 |
| | Negative regulation of microtubule polymerization | 0.02375 |
| | Negative regulation of catenin imports into nucleus | 0.02375 |
| | Sarcoplasmic reticulum calcium ion transport | 0.02375 |
| | Negative regulation of chromatin silencing | 0.02375 |
| | Regulation of actin filament-based movement | 0.02609 |
| | Positive regulation of actin filament depolymerization | 0.02843 |
| | Negative regulation of bone mineralization | 0.02843 |
| | Positive regulation of heterotypic cell-cell adhesion | 0.02843 |
| | Regulation of Wnt signalling pathway | 0.02869 |
| | Protein import into peroxisome matrix | 0.03076 |
| | Collagen metabolic process | 0.03076 |
| | Positive regulation of interleukin-1 production | 0.03076 |
| | Positive regulation of potassium ion transmembrane transporter activity | 0.03076 |
| | Kinetochore organization | 0.03076 |
| | Positive regulation of protein depolymerization | 0.03076 |
| | Regulation of interleukin-1 beta production | 0.03309 |
| | Phospholipase C-activating dopamine receptor signalling pathway | 0.03309 |
| | Negative regulation of biomineral tissue development | 0.03541 |
| | Cellular calcium ion homeostasis | 0.03573 |
| | Protein targeting to peroxisome | 0.03773 |
| | Positive regulation of potassium ion transport | 0.03773 |

| | | |
|---|---|---|
| | Positive regulation of stress-activated protein kinase signalling cascade | 0.03773 |
| | Mitotic sister chromatid cohesion | 0.03773 |
| | Microtubule depolymerization | 0.03773 |
| | Positive regulation of potassium ion transmembrane transport | 0.03773 |
| | Non-canonical Wnt signalling pathway | 0.03786 |
| | G-protein coupled acetylcholine receptor signalling pathway | 0.04004 |
| | Dendritic cell chemotaxis | 0.04004 |
| | Negative regulation of NF-kappaB import into nucleus | 0.04004 |
| | Regulation of cell migration | 0.04041 |
| | Positive regulation of cytosolic calcium ion concentration | 0.04113 |
| | Purine-containing compound metabolic process | 0.04235 |
| | Regulation of lamellipodium organization | 0.04235 |
| | Membrane depolarization during cardiac muscle cell action potential | 0.04235 |
| | Positive regulation of monocyte chemotaxis | 0.04235 |
| | Positive regulation of calcium ion transmembrane transporter activity | 0.04235 |
| | Positive regulation of cation transmembrane transport | 0.04235 |
| | Regulation of cytosolic calcium ion concentration | 0.04337 |
| | Cellular response to growth factor stimulus | 0.04451 |
| | Regulation of heterotypic cell-cell adhesion | 0.04694 |
| | Positive regulation of mononuclear cell migration | 0.04694 |
| | Regulation of calcium ion transmembrane transport | 0.04923 |
| **WikiPathway 2019** | ncRNAs involved in Wnt signalling in hepatocellular carcinoma | 0.01814 |
| | Heme Biosynthesis | 0.02140 |
| | LncRNA involvement in canonical Wnt signalling and colorectal cancer | 0.02143 |
| | Cell-type Dependent Selectivity of CCK2R Signalling | 0.03076 |
| | Wnt Signalling | 0.03113 |
| | Role of Osx and miRNAs in tooth development | 0.03541 |
| | Ectoderm Differentiation | 0.04337 |
| | Endoderm Differentiation | 0.04508 |
| | Serotonin Receptor 2 and ELK-SRF/GATA4 signalling | 0.04694 |
| | Mesodermal Commitment Pathway | 0.04857 |
| | Calcium Regulation in the Cardiac Cell | 0.04976 |
| **Kegg 2019 Human** | Retrograde endocannabinoid signalling | 0.00538 |
| | Long-term depression | 0.00913 |
| | Adherens junction | 0.01296 |
| | Synaptic vesicle cycle | 0.01508 |

| | | |
|---|---|---|
| | Cholinergic synapse | 0.02966 |
| | Serotonergic synapse | 0.03015 |
| | Glutamatergic synapse | 0.03064 |
| | Dopaminergic synapse | 0.03948 |
| | Oxidative phosphorylation | 0.04058 |

***Table 6.*** *Alterated pathways in cells treated with CXCL12-β isoform.*

| **LIBRARY** | **STATISTICALLY SIGNIFICANT PATHWAYS IN SAMPLES TREATED WITH CXCL12-β** | **p-value** |
|---|---|---|
| **GO biological Process 2018** | Regulation of response to interferon-gamma | 0.000005 |
| | Regulation of interferon-gamma-mediated signalling pathway | 0.00002 |
| | Interferon-gamma-mediated signalling pathway | 0.000621 |
| | Regulation of cytokine-mediated signalling pathway | 0.00127 |
| | Cellular response to interferon-gamma | 0.00262 |
| | Positive regulation of calcium ion transport | 0.002890 |
| | Positive regulation of exocytosis | 0.003061 |
| | Sodium ion transmembrane transport | 0.003416 |
| | Interleukin-12-mediated signalling pathway | 0.005463 |
| | Cellular response to interleukin-12 | 0.005463 |
| | Positive regulation of ion transport | 0.005463 |
| | Regulation of calcium ion transport | 0.006901 |
| | Positive regulation of tyrosine phosphorylation of STAT protein | 0.007156 |
| | Regulation of tyrosine phosphorylation of STAT protein | 0.009345 |
| | Positive regulation of JAK-STAT cascade | 0.01023 |
| | Extrinsic apoptotic signalling pathway | 0.01116 |
| | Regulation of phosphatidylinositol 3-kinase signalling | 0.01557 |
| | Apoptotic process | 0.01717 |
| | Positive regulation of cellular component biogenesis | 0.01820 |
| | Calcium ion homeostasis | 0.01820 |
| | Regulation of interleukin-23 production | 0.01865 |
| | Cellular ion homeostasis | 0.01865 |
| | Positive regulation of killing of cells of other organism | 0.01865 |
| | Regulation of cell-cell adhesion mediated by integrin | 0.01865 |
| | Transepithelial transport | 0.02096 |
| | Regulation of protein ADP-ribosylation | 0.02096 |

| | | |
|---|---|---|
| | Tyrosine phosphorylation of STAT protein | 0.02096 |
| | Positive regulation of smooth muscle cell apoptotic process | 0.02096 |
| | Mature B cell differentiation involved in immune response | 0.02326 |
| | Interleukin-23-mediated signalling pathway | 0.02326 |
| | Regulation of sequestering of calcium ion | 0.02326 |
| | Negative regulation of interleukin-17 production | 0.02326 |
| | Regulation of actin filament-based movement | 0.02555 |
| | Wnt signalling pathway | 0.02759 |
| | Interleukin-35-mediated signalling pathway | 0.02785 |
| | Interleukin-27-mediated signalling pathway | 0.02785 |
| | Negative regulation of epithelial cell differentiation | 0.03013 |
| | Positive regulation of potassium ion transmembrane transporter activity | 0.03013 |
| | Regulation of protein import into nucleus, translocation | 0.03013 |
| | Regulation of protein glycosylation | 0.03013 |
| | Establishment of apical/basal cell polarity | 0.03013 |
| | Epithelium development | 0.03043 |
| | Calcium ion transport | 0.03189 |
| | Protein localization to endoplasmic reticulum | 0.03241 |
| | Cellular calcium ion homeostasis | 0.03438 |
| | Negative regulation of biomineral tissue development | 0.03469 |
| | Regulation of extracellular matrix disassembly | 0.03469 |
| | Interleukin-6-mediated signalling pathway | 0.03469 |
| | Mitotic sister chromatid cohesion | 0.03696 |
| | JAK-STAT cascade involved in growth hormone signalling pathway | 0.03696 |
| | Positive regulation of regulated secretory pathway | 0.03922 |
| | Regulation of receptor recycling | 0.04148 |
| | Positive chemotaxis | 0.04148 |
| | Membrane depolarization during cardiac muscle cell action potential | 0.04148 |
| | Positive regulation of monocyte chemotaxis | 0.04148 |
| | Positive regulation of calcium ion transmembrane transporter activity | 0.04148 |
| | Positive regulation of cation transmembrane transport | 0.04148 |
| | Inorganic cation transmembrane transport | 0.04340 |
| | Regulation of epithelial cell differentiation | 0.04374 |
| | Actin filament polymerization | 0.04374 |
| | Regulation of cardiac muscle cell membrane repolarization | 0.04374 |
| | Establishment or maintenance of apical/basal cell polarity | 0.04374 |

| | | |
|---|---|---|
| | Regulation of calcium ion transmembrane transport | 0.04823 |
| **WikiPathway 2019** | Selective expression of chemokine receptors during T-cell polarization | 0.000042 |
| | Type II interferon signalling (IFNG) | 0.000089 |
| | The human immune response to tuberculosis | 0.00132 |
| | RIG-I-like Receptor Signalling | 0.00877 |
| | Human Thyroid Stimulating Hormone (TSH) signalling pathway | 0.01054 |
| | Selenium Micronutrient Network | 0.01743 |
| | ncRNAs involved in Wnt signalling in hepatocellular carcinoma | 0.01743 |
| | LncRNA involvement in canonical Wnt signalling and colorectal cancer | 0.02060 |
| | Heme Biosynthesis | 0.02096 |
| | GPCRs, Class A Rhodopsin-like | 0.02245 |
| | Wnt Signaling WP428 | 0.02995 |
| | ncRNAs involved in STAT3 signalling in hepatocellular carcinoma WP4337 | 0.03013 |
| | Leptin Insulin Overlap WP3935 | 0.03922 |
| | Brain-Derived Neurotrophic Factor (BDNF) signalling pathway WP2380 | 0.04507 |
| | Hypertrophy Model WP516 | 0.04599 |
| **Kegg 2019 Human** | Influenza A | 0.00069 |
| | Th1 and Th2 cell differentiation | 0.00131 |
| | Th17 cell differentiation | 0.002034 |
| | Toxoplasmosis | 0.002376 |
| | Necroptosis | 0.006516 |
| | JAK-STAT signalling pathway | 0.006516 |
| | Tuberculosis | 0.008565 |
| | Inflammatory bowel disease (IBD) | 0.01023 |
| | Salmonella infection | 0.01743 |
| | HIF-1 signalling pathway | 0.02312 |
| | Chagas disease (American trypanosomiasis) | 0.02443 |
| | Herpes simplex virus 1 infection | 0.02807 |
| | Cytokine-cytokine receptor interaction | 0.03170 |
| | Pathways in cancer | 0.03548 |
| | Osteoclast differentiation | 0.03591 |
| | Natural killer cell mediated cytotoxicity | 0.03799 |
| | Signalling pathways regulating pluripotency of stem cells | 0.04230 |

***Table 7.*** *Alterated pathways in cells treated with CXCL12-γ isoform.*

| LIBRARY | STATISTICALLY SIGNIFICANT PATHWAYS IN SAMPLES TREATED WITH CXCL12-γ | p-value |
|---|---|---|
| GO biological Process 2018 | Regulation of catenin import into nucleus | 0.00043 |
| | Positive regulation of calcium ion transport | 0.00126 |
| | Positive regulation of ion transport | 0.00240 |
| | Regulation of calcium ion transport | 0.003050 |
| | Mitotic sister chromatid segregation | 0.007318 |
| | Calcium ion homeostasis | 0.008193 |
| | Cellular metal ion homeostasis | 0.009879 |
| | Nucleus localization | 0.01080 |
| | Cellular divalent inorganic cation homeostasis | 0.01088 |
| | Marginal zone B cell differentiation | 0.01234 |
| | Wnt signalling pathway | 0.01256 |
| | Calcium ion transport | 0.01459 |
| | Regulation of sequestering of calcium ion | 0.01540 |
| | Negative regulation of mitotic nuclear division | 0.01540 |
| | Negative regulation of microtubule polymerization | 0.01540 |
| | Negative regulation of catenin imports into nucleus | 0.01540 |
| | Cellular calcium ion homeostasis | 0.01577 |
| | G-protein coupled receptor signalling pathway | 0.01625 |
| | Regulation of actin filament-based movement | 0.01692 |
| | Negative regulation of bone mineralization | 0.01845 |
| | Regulation of mitotic centrosome separation | 0.01845 |
| | Positive regulation of potassium ion transmembrane transporter activity | 0.01997 |
| | Regulation of ventricular cardiac muscle cell membrane repolarization | 0.02301 |
| | Negative regulation of biomineral tissue development | 0.02301 |
| | Regulation of response to interferon-gamma | 0.02301 |
| | Protein stabilization | 0.02338 |
| | Positive regulation of viral release from host cell | 0.02452 |
| | Positive regulation of potassium ion transport | 0.02452 |
| | Mitotic sister chromatid cohesion | 0.02452 |
| | Microtubule depolymerization | 0.02452 |
| | Positive regulation of potassium ion transmembrane transport | 0.02452 |
| | Dendritic spine morphogenesis | 0.02604 |
| | G-protein coupled acetylcholine receptor signalling pathway | 0.02604 |

| | | |
|---|---|---|
| | Neuron projection development | 0.02781 |
| | Negative regulation of microtubule depolymerization | 0.02906 |
| | Porphyrin-containing compound biosynthetic process | 0.02906 |
| | Acetylcholine receptor signalling pathway | 0.03056 |
| | Regulation of protein kinase A signalling | 0.03056 |
| | Regulation of calcium ion transmembrane transport | 0.03207 |
| | Negative regulation of protein depolymerization | 0.03207 |
| | Regulation of cardiac muscle contraction by calcium ion signalling | 0.03357 |
| | Activation of phospholipase C activity | 0.03507 |
| | Regulation of interferon-gamma-mediated signalling pathway | 0.03507 |
| | Regulation of monocyte chemotaxis | 0.03507 |
| | Negative regulation of protein polymerization | 0.03507 |
| | Regulation of microtubule depolymerization | 0.03507 |
| | Negative regulation of protein imports into nucleus | 0.03507 |
| | Protein localization to cell surface | 0.03507 |
| | Cellular response to nerve growth factor stimulus | 0.03507 |
| | Positive regulation of ion transmembrane transporter activity | 0.03657 |
| | Neuronal action potential | 0.03657 |
| | Microtubule polymerization or depolymerization | 0.03657 |
| | Regulation of cardiac muscle cell action potential | 0.03806 |
| | Dendritic spine organization | 0.03806 |
| | Positive regulation of microtubule polymerization or depolymerization | 0.03806 |
| | Positive regulation of calcium ion transmembrane transport | 0.03955 |
| | Regulation of protein import into nucleus | 0.03955 |
| | Regulation of potassium ion transmembrane transporter activity | 0.03955 |
| | Negative regulation of microtubule polymerization or depolymerization | 0.04253 |
| | Regulation of calcium ion transmembrane transporter activity | 0.04253 |
| | Regulation of canonical Wnt signalling pathway | 0.04325 |
| **WikiPathway 2019** | Selective expression of chemokine receptors during T-cell polarization WP4494 | 0.00091 |
| | ncRNAs involved in Wnt signalling in hepatocellular carcinoma WP4336 | 0.00783 |
| | LncRNA involvement in canonical Wnt signalling and colorectal cancer WP4258 | 0.0093 |
| | Wnt Signalling WP428 | 0.01367 |
| | Heme Biosynthesis WP561 | 0.01387 |
| | Cell-type Dependent Selectivity of CCK2R Signalling WP3679 | 0.01997 |
| | Serotonin Receptor 2 and ELK-SRF/GATA4 signalling WP732 | 0.03056 |
| | Fatty Acid Biosynthesis WP357 | 0.03357 |

| | | |
|---|---|---|
| | The human immune response to tuberculosis WP4197 | 0.03507 |
| | Lipid Metabolism Pathway WP3965 | 0.04402 |
| | Dopaminergic Neurogenesis WP2855 | 0.04550 |
| | Ethanol effects on histone modifications WP3996 | 0.04698 |
| | Gastric Cancer Network 2 WP2363 | 0.04698 |
| **Kegg 2019 Human** | Melanogenesis | 0.01067 |
| | Chagas disease (American trypanosomiasis) | 0.01108 |
| | Retrograde endocannabinoid signalling | 0.02198 |
| | Cushing syndrome | 0.02396 |
| | Wnt signalling pathway | 0.02482 |
| | Alzheimer disease | 0.02873 |
| | Huntington disease | 0.03587 |
| | Proteoglycans in cancer | 0.03862 |
| | Rap1 signalling pathway | 0.04037 |
| | Glyoxylate and dicarboxylate metabolism | 0.04550 |
| | Human cytomegalovirus infection | 0.04732 |
| | Pathways in cancer | 0.04806 |
| | Propanoate metabolism | 0.04846 |

Through this analysis it was observed that treating pancreatic pre-tumour cells (h-Tert-HPNE) with the three different CXCL12 isoforms, many signalling pathways are altered, such as the signalling pathways related to the organization of cytoskeleton, to control the intracellular ionic balance, to chemotaxis, or to other cellular processes such as adhesion, migration and angiogenesis.

In particular, all three isoforms induced a modification in the WNT signalling pathway, both canonical (WNT / β-catenin) and non-canonical (WNT-PCP and WNT-Ca2 +). Processes like cell differentiation during embryogenesis, cell migration, paracrine cell communication and control of homeostasis, are regulated by this signalling pathway. Therefore, WNT plays a crucial role in the mechanisms of cell growth and development [58]. The alteration of this pathway leads to numerous cellular imbalances and is related to the human cancer onset [59, 60].

WNT2B, (Wnt family member 2B), NLK (Nemo Like Kinase) and SFRP5 (Secreted Frizzled Related Protein 5) are the three genes found to be particularly involved in the alteration of the WNT pathway, following treatments with CXCL12 isoforms.

In addition to WNT, the pathways involved in cell migration processes were also found to be altered following treatments with CXCL12-α, CXCL12-β and CXCL12-γ. In all three samples treated, the

over-expression of the CCR1 gene was identified as responsible for this pathway alteration. Between the three samples, the CXCL12-α treated was the one with most statistically significant values (FC = 1.63). It is important to consider that an alteration in epithelial cells migration, not tumoral, is quite unusual. In fact, usually, these pathways are found to be altered in tumour cell lines or in cells that acquire tumour characteristics, such as migration capacity.

In addition to the CCR1 gene, the sample treated with CXCL12-α also showed a down-regulation of the FMN1 gene, related to a reduced expression of E-cadherin. These proteins in physiological condition are expressed by epithelial cells and mediate adhesion between cells in presence of calcium. During a pathological condition or an epithelial to mesenchymal (EMT) transition, expression values of these proteins decreases, therefore they are considered as important markers in tumour transformation processes. Therefore, the α-isoform seems to have a pro-tumour role if administered to pancreatic epithelial cells h-Tert HPNE, as confirmed both by the decrease of the E-cadherin expression and by the over-expression of the CCR1 gene, correlated to a higher cell migration capacity.

From the functional analysis of sample treated with CXCL12-β isoform, alterations in Interferon-γ (FC = 1.51) and apoptosis processes pathways were observed. Treatment with CXCL12-γ isoform also induced an alteration of the Interferon-γ pathway (FC = 1.51), in addition to the alteration of chemotaxis pathway.

### 4.1.6 RT-qPCR

The Real-Time PCR was performed in order to validate the data obtained from the microarray analysis. However, many problems related to the experimental conditions of each primer were encountered. In particular, the problems concerned the primers concentration and the optimal annealing temperatures, in order to obtain reliable and reproducible data. Unfortunately, out of 20 primers pairs purchased, it was possible to successfully perform RT-PCR only for the following 3 genes: DPP4, PTPRB2 and EZH2. The GAPDH housekeeping gene was chosen to normalize the data.

***Table 8*** *Quantification of DPP4, PTPRB and EZH2 transcripts. The ΔCT value corresponds to the difference of the Ct values between the target gene of each sample and the GAPDH of the same sample. The ΔΔCT is instead obtained from the difference between ΔCT of the treated sample and CT of the control. The value obtained is subsequently reported in exponential form (n-fold) according to the formula 2-ΔΔCT.*

DPP4

| | DPP4 | GAPDH | ΔCt | ΔΔCt | n-fold |
|---|---|---|---|---|---|
| CTR | 23,07±0,19 | 15,33±0,49 | 7,73±0,14 | 0±0,14 | 1 (0,90-1.10) |
| CXCL12- α | 23,02±0,24 | 16,93±0,01 | 6,08±0,03 | -1,65±0,03 | 3,13 (3,07-3,20) |
| CXCL12-β | 24,33±0,03 | 15,4±0,2 | 8,93±0,02 | 1,19±0,02 | 0,43 (0,42-0,44) |
| CXCL12-γ | 22,1±0,48 | 16,64±0,003 | 5,46±0,11 | -2,26±0,11 | 4,81 (4,43-5,22) |

PTPRB

| | PTPRB | GAPDH | ΔCt | ΔΔCt | n-fold |
|---|---|---|---|---|---|
| CTR | 31,51±0,13 | 15,33±0,49 | 16,17±0,13 | 0±0,13 | 1 (0,91-1,09) |
| CXCL12- α | 28,7±0,01 | 16,93±0,01 | 11,76±0,00 | -4,4±0,00 | 21,22 (21,22-21,23) |
| CXCL12-β | 29,63±0,31 | 15,4±0,2 | 14,22±0,07 | -1,95±0,07 | 3,86 (3,68-4,05) |
| CXCL12-γ | 34,71±1,07 | 16,64±0,003 | 18,07±0,57 | 1,89±0,57 | 0,26(0,18-0,40) |

EZH2

| | DPP4 | GAPDH | ΔCt | ΔΔCt | n-fold |
|---|---|---|---|---|---|
| CTR | 24,81±0,19 | 15,33±0,49 | 9,47±0,14 | 0±0,14 | 1 (0,9-1,1) |
| CXCL12- α | 25,06±0,9 | 16,93±0,01 | 8,12±0,004 | -1,35±0,004 | 2,55 (2,54-2,56) |
| CXCL12-β | 25,94±0,23 | 15,4±0,2 | 10,53±0,05 | 1,05±0,05 | 0,48 (0,46-0,49) |
| CXCL12-γ | 26,78±0,29 | 16,64±0,003 | 10,14±0,04 | 0,66±0,04 | 0,63 (0,62-0,61) |

Data obtained from RT-PCR, shown that the sample treated with the α-isoform presents a greater quantity of PTPRB transcript compared to the sample treated with the β-isoform. Instead, treatment with the γ-isoform decreased the PTPRB gene expression. Compared to control sample, DPP4 gene is significantly increased in cells exposed to CXCL12-α and CXCL12-γ, while in those exposed to CXCL12-β it is halved. For the EZH2 gene, the amplification showed that treatment with CXCL12-α induced a transcript increase of 2.55 times higher than the control. Instead, EZH2 decreased upon treatment with CXCL12-β and CXCL12-γ.

Finally, to find a correlation between Microarray and RT-PCR data, the fold change values of both methods were compared and for each CXCL12 isoform the correlation coefficient (R2) was evaluated. This R2 factor is comprised between -1 and +1: if the value is greater than 0 it indicates that there is a correlation between the matrices of the data compared, otherwise there is no correlation if the value is less than 0. From this correlation analysis we obtained good correlation coefficient only for CXCL12-γ and not for CXCL12-α and CXCL12-β. However, further tests are needed to obtain more statistically significant data.

### 4.2 Exosomes Analysis

The expression levels of different exosomes populations present in blood of patients with pancreatic ductal adenocarcinoma, were evaluated using the ELISA assay. Blood samples were taken before (time T0) and after three months (time T3) from the first chemotherapy treatment. Out of 19 patients enrolled, 18 of them showed significant results. Unfortunately, due to the progression of the disease and subsequent death, T3 blood sample was possible only for 15 patients. As listed in table 9 and 10, the exosomes carrying the following ubiquitous markers were measured: CD9, CD81, CD44v6, Tsapn8, EpCAM, CD24, CXCR4, the Integrins a6 and b4, and CD133. The values shown are those of sample absorbance measured at 450nm, multiplied by 1000 and normalized for blank value. For those markers it was possible to make a correlation with patients' clinical characteristics. Since CD151, Caveolin-1, PD-L1, Alix, CD133 and Fibronectin were not analysed in all enrolled patients, the correlation between clinical features and these markers was not performed.

***Table 9.*** *Exosome expression level at T0 time point, before the chemotherapy treatment [39].*

| T0 Time point | | | | | | | | | | |
|---|---|---|---|---|---|---|---|---|---|---|
| Pts | CD44 | CD44v6 | CD24 | CD9 | CD81 | EpCAM | Integrin α6 | Integrin β4 | Tspan8 | CXCR4 |
| 1 | 3.6 | 2.1 | 2.3 | 14.5 | 3.4 | 3.2 | 9.6 | 2.4 | 1.7 | 5.2 |
| 2 | 4.9 | 4.5 | 4.6 | 5.5 | 4.7 | 6.3 | 5.7 | 5.3 | 4.2 | 5.5 |
| 3 | 2.5 | 1.6 | 1.8 | 6.2 | 2.8 | 2.5 | 3.9 | 1.8 | 1.4 | 5.1 |
| 4 | 3.4 | 2.0 | 2.1 | 8.3 | 3.5 | 2.9 | 3.3 | 2.3 | 1.9 | 5.3 |
| 5 | 3.3 | 2.5 | 4.3 | 18.6 | 3.0 | 21.4 | 4.4 | 6.5 | 1.9 | 17.5 |
| 6 | 2.6 | 3.6 | 2.6 | 26.5 | 5.1 | 1.2 | 2.5 | 2.8 | 1.8 | 5.9 |
| 7 | 4.0 | 3.6 | 2.8 | 35.5 | 14.7 | 1.0 | 2.1 | 3.0 | 1.7 | 8.7 |
| 8 | 7.6 | 2.7 | 8.3 | 13.9 | 8.9 | 8.3 | 2.8 | 3.0 | 3.0 | 3.8 |
| 10 | 8.0 | 3.1 | 2.9 | 11.2 | 9.8 | 2.1 | 7.0 | 3.4 | 1.7 | 9.1 |
| 11 | 4.0 | 2.2 | 3.5 | 17.9 | 5.8 | 2.8 | 2.3 | 1.8 | 2.2 | 2.5 |
| 12 | 3.3 | 1.5 | 1.5 | 10.3 | 4.4 | 1.2 | 8.7 | 1.9 | 0.9 | 8.1 |
| 13 | 2.6 | 3.5 | 6.3 | 15.9 | 6.6 | 1.4 | 1.5 | 1.7 | 1.8 | 1.5 |
| 14 | 1.1 | 1.3 | 5.3 | 19.7 | 12.4 | 2.0 | 1.5 | 1.0 | 1.0 | 2.2 |
| 15 | 7.8 | 1.3 | 3.1 | 7.3 | 5.8 | 2.2 | 1.3 | 1.1 | 1.3 | 2.6 |
| 16 | 9.2 | 2.0 | 10.2 | 26.3 | 8.4 | 2.6 | 2.6 | 1.5 | 1.2 | 2.9 |
| 17 | 3.9 | 1.9 | 6.1 | 22.5 | 3.8 | 3.3 | 1.8 | 1.2 | 2.1 | 2.7 |
| 18 | 7.5 | 2.9 | 3.4 | 33.2 | 10.1 | 3.4 | 3.7 | 5.7 | 2.2 | 4.4 |
| 19 | 8.2 | 3.5 | 6.2 | 32.9 | 8.9 | 6.3 | 4.8 | 5.5 | 3.7 | 5.0 |

***Table 10.*** *Exosome expression level at T3 time point, after three months from the first chemotherapy treatment [39].*

| T3 Time point | | | | | | | | | | |
|---|---|---|---|---|---|---|---|---|---|---|
| Pts | CD44 | CD44v6 | CD24 | CD9 | CD81 | EpCAM | Integrin α6 | Integrin β4 | Tspan8 | CXCR4 |
| 1 | 3.9 | 2.0 | 2.6 | 12.0 | 2.4 | 17.1 | 3.7 | 5.3 | 1.4 | 17.2 |
| 2 | 6.2 | 5.1 | 4.7 | 10.5 | 4.9 | 20.7 | 6.1 | 11.2 | 2.9 | 17.6 |
| 3 | 3.4 | 1.7 | 3.2 | 7.3 | 3.6 | 16.3 | 2.5 | 4.8 | 1.4 | 15.3 |
| 4 | 2.7 | 2.0 | 2.7 | 13.9 | 3.1 | 13.5 | 4.0 | 4.4 | 1.3 | 14.8 |
| 5 | 2.1 | 5.4 | 3.0 | 26.8 | 5.3 | 1.7 | 1.6 | 1.0 | 3.4 | 8.0 |
| 6 | 3.5 | 4.1 | 1.8 | 32.1 | 4.7 | 2.4 | 1.8 | 1.1 | 1.8 | 6.8 |
| 7 | 5.2 | 1.9 | 1.8 | 12.6 | 5.7 | 1.3 | 5.3 | 1.9 | 0.9 | 8.4 |
| 8 | NA | NA | NA | NA | NA | NA | NA | NA | NA | NA |
| 10 | 11.9 | 4.0 | 4.1 | 10.8 | 11.4 | 1.3 | 3.6 | 3.0 | 3.0 | 3.3 |
| 11 | NA | NA | NA | NA | NA | NA | NA | NA | NA | NA |
| 12 | 2.0 | 2.6 | 2.0 | 4.9 | 2.6 | 2.0 | 0.9 | 4.3 | 2.1 | 1.1 |
| 13 | 4.6 | 3.3 | 7.1 | 30.0 | 8.9 | 2.0 | 1.1 | 1.7 | 2.2 | 1.8 |
| 14 | 1.9 | 3.3 | 2.8 | 15.1 | 4.6 | 1.4 | 1.5 | 1.4 | 1.5 | 1.4 |
| 15 | NA | NA | NA | NA | NA | NA | NA | NA | NA | NA |
| 16 | 4.0 | 3.1 | 7.1 | 21.4 | 5.5 | 1.8 | 2.3 | 2.0 | 2.6 | 1.9 |
| 17 | 3.1 | 4.3 | 9.1 | 19.5 | 7.3 | 2.3 | 3.3 | 1.6 | 3.2 | 2.1 |
| 18 | 6.5 | 2.8 | 4.8 | 23.1 | 9.7 | 4.4 | 6.2 | 5.2 | 3.5 | 3.9 |
| 19 | 7.5 | 3.0 | 5.2 | 30.5 | 8.4 | 5.6 | 5.9 | 4.6 | 3.7 | 4.4 |

The different expression values of exosomal proteins (CD9, CD81, EpCAM, Integrin α6, Integrin β4, CD44, CD44v6, CXCR4, TSPAN8), evaluated on samples at time T0, were used as stratification factors in hierarchical clustering analysis. Through this analysis, three different clusters were identified, as shown in following figure.

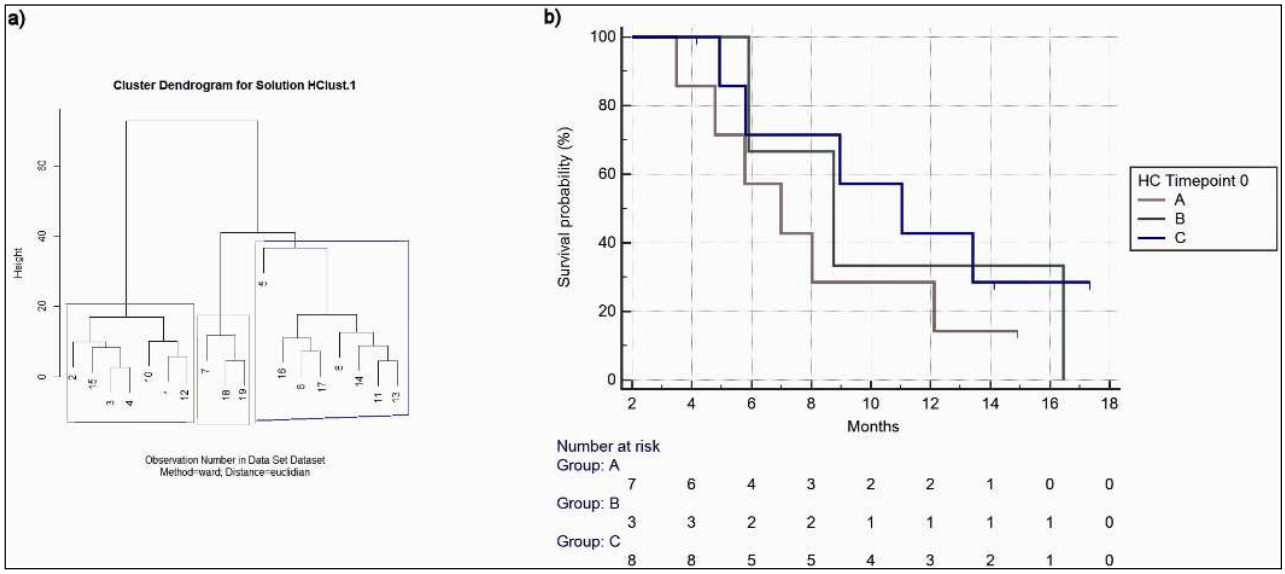


***Figure 9.*** *Hierarchical clustering analysis at time point T0. a) cluster dendrogram; b) overall survival between clusters [39].*

K-means analysis (K = 3 means 3 different clusters) was performed to identify the key determinants of different distribution among the groups. It has recognized the expression of CD9 and CD81 as key factor in one group, whereas other group's distribution was determined by expression of EpCAM and CXCR4 (with minor role of Integrin α6 and β4). Different expression of CD44, CD24, CD44v6, TSPAN8 did not influence distribution among three different groups.

The same analysis was used for the expression values of exosomal proteins in the samples at time point T3. The results obtained were the same as at the ones for the time point T0, where: the first group included CD9 and CD81, the second EpCAM and CXCR4, while the third group, more marginal group, Integrin α6 and Integrin β4.

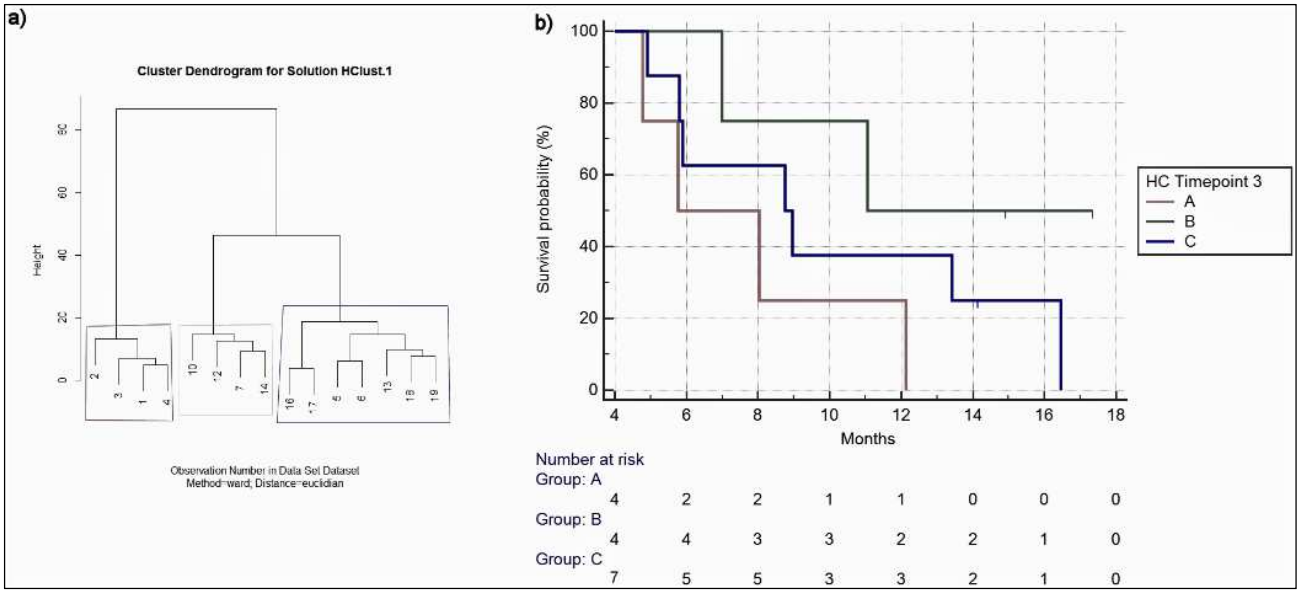


***Figure 10.*** *Hierarchical clustering analysis at time point T3. a) cluster dendrogram; b) overall survival between clusters [39].*

Based on this observed cluster division, three different analyses were carried out in order to correlate the exosomes expression levels with clinical outcomes of different patients. As a first analysis, PFS (the time elapsed between the first cycle of chemotherapy and the first radiological progression) values were compared with EpCAM expression levels at T0 time point. A statistically significant correlation was observed with worse PFS: patients expressing high EpCAM values had a median PFS of 3. 18 months compared to patients with lower EpCAM values where it was 7. 31 (HR:2. 82, 95% CI:1. 03-7. 73, p=0. 01).

High levels of EpCAM expression also correlated with shorter patient overall survival (OS) (the time elapsed between the first cycle of chemotherapy and the patient's death) (5. 83 vs 16. 45 months, HR:6. 16, 95%CI:1. 93-19. 58, p = 0. 0001) and lower response rate (20% vs 87%). Similarly, at T3 time point, high levels of EpCAM expression correlated with worse OS, shorter PFS and response rates of 33% compared to 67%. However, these differences were not statistically significant. Regarding CXCR4, CD9 and CD81 markers, both T0 and T3 time point, there were no differences in terms of OS and PFS. The response rates between high and low expression levels were 50% vs 50% for CXCR4 and CD9, CD81 shown respectively 66% vs 33%, but it was not statistically significant.

In a second analysis, it was evaluated whether the various patients grouped in different clusters presented different clinical outcomes. At time T0 three different OSs were observed (6. 98 vs 8. 75 vs 11. 04 months) but were not statistically significant. Performing the analysis on the samples at time point T3, the differences were more evident (5. 77 vs 11. 04 vs 8. 75 months) but still not significant.

Finally, the third analysis, was carried out to assess whether the increase or decrease in exosomal protein expression values, between time T0 and time T3, can be useful to understand the patients' outcome. Analysing percentage variations between time T0 and T3, the EpCAM increase was found to be related to better PFS and OS. Patients with increased levels of EpCAM showed also a higher response rate (60%) than those with a lower expression level (20%).

## 5. DISCUSSIONS AND CONCLUSIONS

The growing number of studies of the pancreatic cancer microenvironment showed that it is widely involved in the development and progression of tumour. In fact, the interaction that takes place between tumour and stromal cells due to the release of growth factors, chemokines and exosomes, promotes the maintenance and the constant feeding of this particular type of tumour. Nowadays, numerous studies have not yet explained the complex role both of each chemokine CXCL12 isoform released in the pancreatic tumour microenvironment and of the many exosomes released by all cells at different times and with different cargo.

### CXCL12

In order to shed light on the role of each CXCL12 isoform related to PDAC, in this work I evaluated the effect of the three commercially available isoforms, CXCL12-α, CXCL12-β and CXCL12-γ, on the pancreatic pre-tumour cell line h-TERT HPNE. In literature there are contrasting opinions regarding role of these proteins, for example, according to some the CXCL12-α isoform plays a pro-tumour role favouring pancreatic cancer growth and development [32, 61], according to others, re-expression of this chemokine may induce a decrease in pancreatic cancer growth and migration [62]. Until now, in numerous papers published, authors have not specified which isoforms have been investigated, therefore, this discordance regarding the different CXCL12 roles could indicate a specific role for each isoform. In this work, in order to investigate how each CXCL12 isoform takes part in the mechanisms of development of pancreatic cancer, the effects of treatments with each isoform on the h-Tert HPNE pro tumour cell line have been evaluated by means of western blot, wound healing assay, soft agar and microarray analysis. Only the α and β isoforms could have been used for protein expression analysis, as the isoform-γ was later purchased. This analysis showed that in both cases, either by treating the cells with α-isoform or with the β-isoform, there is an increase in expression of the mesenchymal markers Vimentin and N-cadherin. The alteration of both factors is indicator of epithelial to mesenchymal transition (EMT), although, as regards the E-cadherin epithelial marker, this has not been found in our control cells (cells that have not received the treatment with the CXCL12-isoforms). We hypothesized that this phenomenon could be due to the presence of the Kras gene modification in our h-Tert HPNE cell line. As for the increase in mesenchymal markers expression, CXCL12-α gave higher expression values in our cells compared to β-isoform. The latter has a greater pro-tumour potential to induce a slight increase in the CD44 stem marker. Both isoforms also induce activation of mTOR and ERK pathways, in particular, CXCL12-β shows a greater ability to induce ERK phosphorylation, compared to CXCL12-α. From data obtained by the migration assay, CXCL12-α treatments, compared to those with CXCL12-β, seem to induce a higher migration rate in h-Tert HPNE cells. Instead, for the purpose of whole transcriptome analysis, the effects of the three commercially available isoforms were investigated:

CXCL12-α, CXCL12-β and CXCL12-γ. Through Microarray analysis, we observed an alteration of the gene expression profile following treatments with each of the three CXCL12-isoforms. From this analysis it emerged that upon treatments with the α-isoform, cells showed an alteration in migration, proliferation and inflammation pathways, suggesting that this treatment induces an epithelial to mesenchymal transition in the hTERT-HPNE cells (EMT). As for the other two isoforms, CXCL12-β and CXCL12-γ, we have no obvious data on this. From the first Real-Time PCR data obtained, a partial correlation was observed only in the sample treated with CXCL12-γ. However, these data are not statistically sufficient for validating the Microarray analysis. It will be necessary to proceed with the quantification, via Real-Time PCR, of the transcripts of at least 20 genes selected by the Microarray.

In conclusion, this work demonstrates that both CXCL12-α and CXCL12-β show a pro-tumour effect on the pancreatic pre-tumour cell line h-Tert HPNE, as they induce an alteration in some pathways involved in tumorigenesis processes of pancreatic cancer. However, from data obtained by the soft agar assay, the treatment for only 24h is not sufficient to induce a neoplastic transformation in these cells. Therefore, the use of prolonged treatments could be useful to define this aspect. Finally, future studies could be directed to establish the role of the other CXCL12 isoforms not yet studied, in order to suggest potential therapeutic strategies for the PDAC treatment.

**EXOSOMES**

One of the most common problems found in pancreatic cancer is to identify plasma markers specific to the early tumour stages. For this reason, in recent years, the growing interest in this field has focused mainly on exosomes. Exosomes are alternative biomarkers, easily available through liquid biopsy. Thanks to the specific proteins present on their surface, it is in fact possible to distinguish exosomes origin from different populations of cancer cells. In this work, I analysed PDAC plasma samples in order to identify a correlation between the different types of exosomes and the clinical data of patients. Through the ELISA assay, previously developed by our group, I evaluated the relative quantities of exosomal tumour markers in patients enrolled before and after chemotherapy treatments. From obtained results it emerged that EpCAM protein (Epithelial cell adhesion molecule) could play an important role as a prognostic factor for pancreatic cancer. EpCAM is a glycoprotein involved in cell-signalling, migration and proliferation. In fact, at T0 time point, higher EpCAM expression levels were found in patients with poor performance status and were associated with worse PFS and OS. Differently, at T3 time point (after chemotherapy treatment), in patients with increased expression levels of EpCAM during treatment, an improvement in PFS and OS was observed. Therefore, from obtained results, although at time T0 high levels of EpCAM are correlated with worse prognosis, in patients in whom increase is found upon chemiotherapy treatment, the prognosis is

actually better. The correlation with the worst prognosis at time T0 of EpCAM's high expression levels is probably due to the high tumour rate of patients at the time of enrolment. However, usually high levels of EpCAM in epithelial cells are associated with an increase in proliferative activity and a decrease in differentiation [63]. In conclusion, further studies will be useful to understand the mechanism underlying the exosomal increase in EpCAM expression levels in patients at time T3.

## 6. REFERENCES


1. Luchini, C., P. Capelli, and A. Scarpa, *Pancreatic Ductal Adenocarcinoma and Its Variants.* Surg Pathol Clin, 2016. **9**(4): p. 547-560.
2. Rawla, P., T. Sunkara, and V. Gaduputi, *Epidemiology of Pancreatic Cancer: Global Trends, Etiology and Risk Factors.* World J Oncol, 2019. **10**(1): p. 10-27.
3. Yamaguchi, J., et al., *Cells of origin of pancreatic neoplasms.* Surg Today, 2018. **48**(1): p. 9-17.
4. Kamisawa, T., et al., *Pancreatic cancer.* Lancet, 2016. **388**(10039): p. 73-85.
5. Satyananda, V., et al., *Advances in Translational Research and Clinical Care in Pancreatic Cancer: Where Are We Headed?* Gastroenterol Res Pract, 2019. **2019**: p. 7690528.
6. Ilic, M. and I. Ilic, *Epidemiology of pancreatic cancer.* World J Gastroenterol, 2016. **22**(44): p. 9694-9705.
7. Padoan, A., M. Plebani, and D. Basso, *Inflammation and Pancreatic Cancer: Focus on Metabolism, Cytokines, and Immunity.* Int J Mol Sci, 2019. **20**(3).
8. Partensky, C., *Toward a better understanding of pancreatic ductal adenocarcinoma: glimmers of hope?* Pancreas, 2013. **42**(5): p. 729-39.
9. Ansari, D., et al., *Proteomic and genomic profiling of pancreatic cancer.* Cell Biol Toxicol, 2019. **35**(4): p. 333-343.
10. Hezel, A.F., et al., *Genetics and biology of pancreatic ductal adenocarcinoma.* Genes Dev, 2006. **20**(10): p. 1218-49.
11. Weber, C.E. and P.C. Kuo, *The tumor microenvironment.* Surg Oncol, 2012. **21**(3): p. 172-7.
12. Gardian, K., et al., *Analysis of pancreatic cancer microenvironment: role of macrophage infiltrates and growth factors expression.* J Cancer, 2012. **3**: p. 285-91.
13. Feig, C., et al., *The pancreas cancer microenvironment.* Clin Cancer Res, 2012. **18**(16): p. 4266-76.
14. Righetti, A., et al., *CXCL12 and Its Isoforms: Different Roles in Pancreatic Cancer?* J Oncol, 2019. **2019**: p. 9681698.
15. Pan, B., et al., *Cancer-associated fibroblasts in pancreatic adenocarcinoma.* Future Oncol, 2015. **11**(18): p. 2603-10.
16. Dougan, S.K., *The Pancreatic Cancer Microenvironment.* Cancer J, 2017. **23**(6): p. 321-325.
17. Awaji, M. and R.K. Singh, *Cancer-Associated Fibroblasts' Functional Heterogeneity in Pancreatic Ductal Adenocarcinoma.* Cancers (Basel), 2019. **11**(3).
18. Daniel, S.K., et al., *Hypoxia as a barrier to immunotherapy in pancreatic adenocarcinoma.* Clin Transl Med, 2019. **8**(1): p. 10.
19. Uzunparmak, B. and I.H. Sahin, *Pancreatic cancer microenvironment: a current dilemma.* Clin Transl Med, 2019. **8**(1): p. 2.
20. Takahashi, K., et al., *Pancreatic tumor microenvironment confers highly malignant properties on pancreatic cancer cells.* Oncogene, 2018. **37**(21): p. 2757-2772.
21. Marcuzzi, E., et al., *Chemokines and Chemokine Receptors: Orchestrating Tumor Metastasization.* Int J Mol Sci, 2018. **20**(1).
22. Janssens, R., S. Struyf, and P. Proost, *The unique structural and functional features of CXCL12.* Cell Mol Immunol, 2018. **15**(4): p. 299-311.
23. Janssens, R., S. Struyf, and P. Proost, *Pathological roles of the homeostatic chemokine CXCL12.* Cytokine Growth Factor Rev, 2018. **44**: p. 51-68.
24. Meng, W., S. Xue, and Y. Chen, *The role of CXCL12 in tumor microenvironment.* Gene, 2018. **641**: p. 105-110.
25. Zhou, Y., et al., *The CXCL12 (SDF-1)/CXCR4 chemokine axis: Oncogenic properties, molecular targeting, and synthetic and natural product CXCR4 inhibitors for cancer therapy.* Chin J Nat Med, 2018. **16**(11): p. 801-810.
26. Zhou, W., et al., *Targeting CXCL12/CXCR4 Axis in Tumor Immunotherapy.* Curr Med Chem, 2019. **26**(17): p. 3026-3041.
27. Teixido, J., et al., *The good and bad faces of the CXCR4 chemokine receptor.* Int J Biochem Cell Biol, 2018. **95**: p. 121-131.

28. Guyon, A., *CXCL12 chemokine and its receptors as major players in the interactions between immune and nervous systems.* Front Cell Neurosci, 2014. **8**: p. 65.
29. Scala, S., *Molecular Pathways: Targeting the CXCR4-CXCL12 Axis--Untapped Potential in the Tumor Microenvironment.* Clin Cancer Res, 2015. **21**(19): p. 4278-85.
30. Luker, K.E., et al., *Constitutive and chemokine-dependent internalization and recycling of CXCR7 in breast cancer cells to degrade chemokine ligands.* Oncogene, 2010. **29**(32): p. 4599-610.
31. Zhao, S., et al., *A Comprehensive Analysis of CXCL12 Isoforms in Breast Cancer(1,2.).* Transl Oncol, 2014.
32. Gosalbez, M., et al., *Differential expression of SDF-1 isoforms in bladder cancer.* J Urol, 2014. **191**(6): p. 1899-1905.
33. Allami, R.H., et al., *Analysis of the expression of SDF-1 splicing variants in human colorectal cancer and normal mucosa tissues.* Oncol Lett, 2016. **11**(3): p. 1873-1878.
34. Jung, Y., et al., *CXCL12gamma Promotes Metastatic Castration-Resistant Prostate Cancer by Inducing Cancer Stem Cell and Neuroendocrine Phenotypes.* Cancer Res, 2018. **78**(8): p. 2026-2039.
35. Bebelman, M.P., et al., *Biogenesis and function of extracellular vesicles in cancer.* Pharmacol Ther, 2018. **188**: p. 1-11.
36. Kowal, J., M. Tkach, and C. Thery, *Biogenesis and secretion of exosomes.* Curr Opin Cell Biol, 2014. **29**: p. 116-25.
37. Batista, I.A. and S.A. Melo, *Exosomes and the Future of Immunotherapy in Pancreatic Cancer.* Int J Mol Sci, 2019. **20**(3).
38. Costa-Silva, B., et al., *Pancreatic cancer exosomes initiate pre-metastatic niche formation in the liver.* Nat Cell Biol, 2015. **17**(6): p. 816-26.
39. Giampieri, R., et al., *Clinical impact of different exosomes' protein expression in pancreatic ductal carcinoma patients treated with standard first line palliative chemotherapy.* PLoS One, 2019. **14**(5): p. e0215990.
40. Richards, K.E., et al., *Cancer-associated fibroblast exosomes regulate survival and proliferation of pancreatic cancer cells.* Oncogene, 2017. **36**(13): p. 1770-1778.
41. Jin, H., et al., *Exosomal zinc transporter ZIP4 promotes cancer growth and is a novel diagnostic biomarker for pancreatic cancer.* Cancer Sci, 2018. **109**(9): p. 2946-2956.
42. Ruivo, C.F., et al., *The Biology of Cancer Exosomes: Insights and New Perspectives.* Cancer Res, 2017. **77**(23): p. 6480-6488.
43. Clark, C.E., et al., *Dynamics of the immune reaction to pancreatic cancer from inception to invasion.* Cancer Res, 2007. **67**(19): p. 9518-27.
44. Ino, Y., et al., *Immune cell infiltration as an indicator of the immune microenvironment of pancreatic cancer.* Br J Cancer, 2013. **108**(4): p. 914-23.
45. Chen, G., et al., *Exosomal PD-L1 contributes to immunosuppression and is associated with anti-PD-1 response.* Nature, 2018. **560**(7718): p. 382-386.
46. Linton, S.S., et al., *Tumor-promoting effects of pancreatic cancer cell exosomes on THP-1-derived macrophages.* PLoS One, 2018. **13**(11): p. e0206759.
47. Au Yeung, C.L., et al., *Exosomal transfer of stroma-derived miR21 confers paclitaxel resistance in ovarian cancer cells through targeting APAF1.* Nat Commun, 2016. **7**: p. 11150.
48. Lan, B., et al., *The Role of Exosomes in Pancreatic Cancer.* Int J Mol Sci, 2019. **20**(18).
49. Kupfer, P., et al., *Batch correction of microarray data substantially improves the identification of genes differentially expressed in rheumatoid arthritis and osteoarthritis.* BMC Med Genomics, 2012. **5**: p. 23.
50. Dave, J.M. and K.J. Bayless, *Vimentin as an integral regulator of cell adhesion and endothelial sprouting.* Microcirculation, 2014. **21**(4): p. 333-44.
51. Sharma, P., et al., *Intermediate Filaments as Effectors of Cancer Development and Metastasis: A Focus on Keratins, Vimentin, and Nestin.* Cells, 2019. **8**(5).
52. Myoteri, D., et al., *Prognostic Evaluation of Vimentin Expression in Correlation with Ki67 and CD44 in Surgically Resected Pancreatic Ductal Adenocarcinoma.* Gastroenterol Res Pract, 2017. **2017**: p. 9207616.
53. Zhao, S., et al., *CD44 Expression Level and Isoform Contributes to Pancreatic Cancer Cell Plasticity, Invasiveness, and Response to Therapy.* Clin Cancer Res, 2016. **22**(22): p. 5592-5604.

54. Li, X.P., et al., *Expression of CD44 in pancreatic cancer and its significance.* Int J Clin Exp Pathol, 2015. **8**(6): p. 6724-31.
55. Durko, L., et al., *Expression and Clinical Significance of Cancer Stem Cell Markers CD24, CD44, and CD133 in Pancreatic Ductal Adenocarcinoma and Chronic Pancreatitis.* Dis Markers, 2017. **2017**: p. 3276806.
56. Lee, H.S., et al., *STMN2 is a novel target of beta-catenin/TCF-mediated transcription in human hepatoma cells.* Biochem Biophys Res Commun, 2006. **345**(3): p. 1059-67.
57. Chen, Y., M. Lohr, and R. Jesnowski, *Inhibition of ankyrin-B expression reduces growth and invasion of human pancreatic ductal adenocarcinoma.* Pancreatology, 2010. **10**(5): p. 586-96.
58. Komiya, Y. and R. Habas, *Wnt signal transduction pathways.* Organogenesis, 2008. **4**(2): p. 68-75.
59. Duchartre, Y., Y.M. Kim, and M. Kahn, *The Wnt signaling pathway in cancer.* Crit Rev Oncol Hematol, 2016. **99**: p. 141-9.
60. MacDonald, B.T., K. Tamai, and X. He, *Wnt/beta-catenin signaling: components, mechanisms, and diseases.* Dev Cell, 2009. **17**(1): p. 9-26.
61. Connell, B.J., et al., *Heparan sulfate differentially controls CXCL12alpha- and CXCL12gamma-mediated cell migration through differential presentation to their receptor CXCR4.* Sci Signal, 2016. **9**(452): p. ra107.
62. Liu, Z., et al., *Expression of stromal cell-derived factor 1 and CXCR7 ligand receptor system in pancreatic adenocarcinoma.* World J Surg Oncol, 2014. **12**: p. 348.
63. Trager, M.M. and S.A. Dhayat, *Epigenetics of epithelial-to-mesenchymal transition in pancreatic carcinoma.* Int J Cancer, 2017. **141**(1): p. 24-32.